ISTANBUL TECHNICAL UNIVERSITY ★ GRADUATE SCHOOL

STIMULI RESPONSIVE SUPRAMOLECULAR POLYMERS AND IDA SENSORS BASED ON HOST-GUEST INTERACTION AND ION PAIR RECOGNITION ABILITY OF CALIX[4]PYRROLES

Ph.D. THESIS

Sana AMHARAR

Department of Chemistry

Chemistry Programme

FEBRUARY 2022

ISTANBUL TECHNICAL UNIVERSITY ★ GRADUATE SCHOOL

STIMULI RESPONSIVE SUPRAMOLECULAR POLYMERS AND IDA SENSORS BASED ON HOST-GUEST INTERACTION AND ION PAIR RECOGNITION ABILITY OF CALIX[4]PYRROLES

Ph.D. THESIS

Sana AMHARAR
(509142012)

Department of Chemistry

Chemistry Programme

Thesis Advisor: Assoc. Prof. Dr. Abdullah AYDOĞAN

FEBRUARY 2022

İSTANBUL TEKNİK ÜNİVERSİTESİ ★LİSANSÜSTÜ EĞİTİM ENSTİTÜSÜ

KALİKS[4]PİROLLERİN EV SAHİBİ-MİSAFİR ETKİLEŞİMİ VE İYON ÇİFTİ TANIMA ÖZELLİĞİ ÜZERİNE OLUŞTURULMUŞ, UYARANLARA DUYARLI SUPRAMOLEKÜLER POLİMERLER VE IDA SENSÖRLERİ

DOKTORA TEZİ

Sana AMHARAR
(509142012)

Kimya Anabilim Dalı

Kimya Programı

Tez Danışmanı: Doç. Dr. Abdullah AYDOĞAN

ŞUBAT 2022

Sana AMHARAR, a Ph.D. student of ITU Graduate School student ID 509142012, successfully defended the thesis entitled "STIMULI RESPONSIVE SUPRAMOLECULAR POLYMERS AND IDA SENSORS BASED ON HOST-GUEST INTERACTION AND ION PAIR RECOGNITION ABILITY OF CALIX[4]PYRROLES" which she prepared after fulfilling the requirements specified in the associated legislations, before the jury whose signatures are below.

Thesis Advisor:	**Assoc.Prof. Dr. Abdullah AYDOĞAN** IstanbulTechnical University	.....
Jury Members:	**Prof. Dr. Gürkan HIZAL** Istanbul Technical University	.....
	Prof. Dr. Hakan DURMAZ Istanbul Technical University	.....
	Assoc. Prof. Dr. Murat ÖZMEN Yıldız Technical University	.....
	Assoc. Prof. Dr. Gökçe MEREY Marmara University	.....

Date of Submission : 23 December 2021
Date of Defense : 7 February 2022

To the AMHARAR clan,

FOREWORD

First of all, I would like to thank to my supervisor Assoc. Prof. Dr. Abdullah AYDOĞAN for his guidance and advises.I will also not forget my collegues who made the Aydoğan laboratory an enjoyfull place.

My second word will be to my dear AMHARAR family those who left us already and those who are present: My father Si Abdulwahid AMHARAR, my mother Aicha Tabendohot AMHARAR and her mother Ima Halima. My sisters and brothers: Najat, Younes, Charifa, Ilyas, Naima, Sarah and Linda, my nephews: Imran, Aadam, Mahlail, Muhammad Aliyy Abdulwahid and the one who doesn't have a name yet.

I also thank The Scientific and Technological Research Council of Turkey (TUBITAK 116Z980) for the financial support.

February 2022

Sana AMHARAR
(M.Sc. Chemist)

TABLE OF CONTENTS

Page

ABBREVIATIONS

^{13}C NMR	**:** Carbon Nuclear Magnetic Resonance Spectroscopy
$CDCl_3$	**:** Deutareted Chloroform
CH_2Cl_2	**:** Dichloromethane
$CHCl_3$	**:** Chloroform
CH_3SO_3H	**:** Methanesulfonic Acid
CNT	**:** Carbon Nano Tube
CPC	**:** Critical Polymerization Concentration
CTA	**:** Cetrimonium cation
CTAOH	**:** Cetrimonium Hyrdroxide
CTAOAc	**:** Cetrimonium Acetate
DCM	**:** Dichloromethane
DOSY	**:** Diffusion-Ordered NMR Spectroscopy
DP	**:** Degree of Polymerization
FT-IR	**:** Fourier Transform Infrared Spectrophotometer
^{1}H-NMR	**:** Hydrogen Nuclear Magnetic Resonance Spectroscopy
MeOH	**:** Methylalcohol
NOESY	**:** Nuclear Overhauser Effect Spectroscopy
ROSY	**:** Relaxation Ordered Spectroscopy
DOESY	**:** Diffusion Ordered Spectroscopy
RT	**:** Room Temperature
SEM	**:** Scanning Electron Microscope
TBA	**:** Tetrabuthylammonium Cation
TBAOH	**:** Tetrabuthylammonium hydroxide
THF	**:** Tetrahydrofurane
Vs	**:** Specific Viscosity

SYMBOLS

Å	**:** Angstrom
λ	**:** Wavelength

LIST OF TABLES

Page

LIST OF FIGURES

Page

STIMULI RESPONSIVE SUPRAMOLECULAR POLYMERS AND IDA SENSORS BASED ON HOST-GUEST INTERACTION AND ION PAIR RECOGNITION ABILITY OF CALIX[4]PYRROLES

SUMMARY

Calix[4]pyrroles are the macrocyclic compounds with four pyrrol units connected to each other via sp^3 carbon atoms. Their anion binding ability in organic solvent has make them gain attention in the sensing area. It is cost-effective, easy to synthesize and to modify. This thesis is divided into four parts, first chapter corresponding to an introduction about generality in supramolecular chemistry and calix[4]pyrroles, and the next three different chaptersare based on the three articles published during this PhD study.

In Chapter 2, supramolecular polymerization of calix[4]pyrroles bearing tethered carboxylate functional groups was reported in the form of their tetrabutylammonium salts. At high concentrations one of the calix[4]pyrroles with a shorter linker between the calixpyrrole core and the carboxylate unit was found to give a thermoresponsive supramolecular polymer gel.

In Chapter 3, rationally designed ion pairs were integrated into a calix[4]pyrrole skeleton, resulting the formation of an ion pair recognition based linear supramolecular polymer. The effect of simultaneous host-guest and cation-π interactions between carboxylate functional calix[4]pyrrole and cetyltrimethylammonium cation was investigated by NMR, viscosity, SEM, and DSC analyses. The resulting supramolecular polymer was found to show temperature induced rapid and reversible sol-gel transition through van der Waals interactions of cetyl units.

And finally in chapter 4, cost-effective fluorescence turn-on indicator-displacement-assay (IDA) sensors based on octamethylcalix[4]pyrrole receptor and tetrabutylammonium salts of 4-methylumbelliferone and fluorescein indicators were developed for highly sensitive detection of fluoride anion. The IDA sensor assembly relies on the hydrogen bonding between calix[4]pyrrole and carboxylate units of indicators and further displacement of receptors with target analyte. While all the sensors displayed rapid and selective sensitivity towards fluoride over the other anions, 4-methylumbelliferone based IDA system was also found to have a visual color change for the sensing of fluoride anion. The experimental results revealed that fluorescein-based IDA sensor could be used for the sensing of fluoride anion with a detection limit as low as 3.2 nM.

KALİKS[4]PİROLLERİN EV SAHİBİ-MİSAFİR ETKİLEŞİMİ VE İYON ÇİFTİ TANIMA ÖZELLİĞİ ÜZERİNE OLUŞTURULMUŞ, UYARANLARA DUYARLI SUPRAMOLEKÜLER POLİMERLER VE IDA SENSÖRLERİ

ÖZET

Kaliks[4]piroller, sp^3 karbon atomları ile birbirine bağlı dört pirol ünitesine sahip makrosiklik bileşiklerdir. Organik çözücüdeki anyon bağlama yetenekleri, sensör kimyasında dikkat çekmelerini sağlamıştır. Düşük maliyetlidir, sentezlenmesi ve fonksiyonlandırılmaları kolaydır. Literatürde, pillararen, siklodekstrin bazlı birçok supramoleküler polimer görebiliriz, katyon bağlama yeteneği üzerine kurulmuş supramoleküler polimer yaygındır.

Kaliks[4]piroller, yaygın aprotik organik çözücülerde (örneğin, $CHCl_3$ ve CH_3CN) anyonları seçici olarak bağlayabilir. İyon seçici optic ve elektro aktif sensörler, anyon özütleyiciler, anyon ayırıcı katı destekler, transmembran iyon taşıyıcılar, moleküler kaplar, ve nanosensörler olarak kullanılmıştır. Çeşitli uygulamalar için geliştirilmiş sistemlere birkaç örnek sayabiliriz. Bununla birlikte, supramoleküler polimer kimyasında kullanımları nadirdir.

Örneğin, supramoleküler düzenekler elde etmek için tetratiafulvalen-fonksiyonelleştirilmiş ve imidazolyum bağlı kaliks[4]piroller kullanılmıştır. Sonuçta ortaya çıkan supramoleküler düzeneklerin dinamik konuk bağımlı yapısal dönüşümlere maruz kaldıklarının bulunmasına rağmen, bu sistemler solüsyonda nispeten düşük derecede supramoleküler polimerizasyon sergilemiştir.

Bu bulgular bizi, tetrapirrolik makrosiklenin güçlü bir şekilde bağlayabileceği, negatif yüklü bir parça taşıyan, hazırlanması kolay, yüksek oranda çözünür heteroditopik kaliks[4]pirol monomerleri tasarlamaya sevk etti.

Kaliks[4]pirollerin anyon bağlama yeteneği üzerine kurulmuş supramoleküler polimerler nadirdir.

Bu çalışmalarımızda, anyon bağlama yeteneğin sayesinde ünik özelliklere sahip supramoleküler polimer elde edilmiştir.

Florür (F^-) bazı yeraltı sularında yüksek seviyelerde bulunur ve bazı psikiyatrik ilaçlar ve anesteziklerde bileşen olarak kullanılır. Yetersiz veya aşırı florür maruziyeti, diş çürümesine, kemik bozukluğuna ve tiroid hastalıklara neden olabilir. Aynı zamanda kimyasal sılahlarında (örneğin Sarin, Tabun ve diizopropilflorofosfat) ve bazı böcek zehirlerinin işlevinde de aktif rollere sahiptir.

Bu nedenle, çeşitli optik olarak aktif kimyasal platformlar aracılığıyla florür iyonunun seçici olarak sensörleri geliştirilmiştir.

Kaliks[4]pirol ve fluorür arasında ki bağlanma sabiti oldukça yüksektir.Bu sebep ile fluorür tespiti için kaliks[4]pirol bazlı sensörler umut vericidir ancak literatürde bulunan kaliks[4]pirol bazlı olan fluorür sensörleri yüksek maliyetlidir, sentezlenmesi zahmetlidir.

Bu sebep ile, piyasada bulunan malzemelerden başlayarak tek bir sentetik adımda hazırlanabilen basit ve uygun maliyetli bir kaliks[4]pirol IDA sensörü tasarlamak ve bu IDA sistemini F^- iyonunun seçici optik algılamasında kullanmak bu çalışmanın amaçları arasındadır.

Bu tez dört bölüme ayrılmıştır.

Birinci bölüm giriş bölümüdür, supramoleküler kimya, supramoleküler polimerler uygulamaları ve avantajları, kaliks[4]piroller ve özellikleri ile ilgili genel bilgiler içermektedir.

Diğer üç bölüm ise bu doktora çalışması sırasında yayınlanan üç makaleye karşılık gelmektedir.

Tezin ikinci bölümünde, karboksilat fonksiyonel grupları taşıyan kaliks[4]pirollerin (tetrabutilamonyum tuzları şeklinde) supramoleküler polimerizasyonu gerçekleştirilmiştir.

Yüksek konsantrasyonlarda, kalikspirol ile karboksilat ünitesi arasında daha kısa mesafeye sahip olan kaliks[4]pirolün sıcaklık değişimine duyarlı bir supramoleküler polimer jele dönüştüğü bulunmuştur.

Bu supramoleküler polimerin karakterizasyonu çeşitli spektroskopik yöntemler ile yapılmıştır (^{1}H-NMR, ^{13}C-NMR, DOSY NMR, NOSY NMR) ve kromatografik-saflaştırma teknikleri uygulanmıştır.

Elde edilen saf supramoleküler jelin ısıya karşı davranışları incelemek için. viskozite ölçümleri yapılmıştır.

Üçüncü bölümünde, rasyonel olarak tasarlanmış iyon çiftleri bir kaliks[4]pirol iskeletine entegre edilmiştir ve iyon çifti tanınmasına dayanarak lineer bir supramoleküler polimer hazırlanmıştır.

Karboksilat fonksiyonel kaliks[4]pirol ve setiltrimetilamonyum arasındaki eşzamanlı evsahibi-misafir ve katyon-π etkileşimleri ve bu etkleşimler sonucunda oluşan supramoleküler polimer NMR, viskozite, SEM ve DSC analizleri ile irdelenmiştir.

Supramoleküler polimerin üzerinde ki rakip anyon (flüorür) etkileri incelenmiştir. ^{1}H-NMR analizler ile ve fotoğralar ile gösterilmiştir.

Elde edilen supramoleküler polimerin, yapısına entegre olmuş setil ünitelerin van der Waals etkileşimleri sayesindeısıyaduyarlı hızlı ve tersine çevirilebilir sol-jel geçişi gösterdiği bulunmuştur. Bu sol-jel geçiçin incelenmesi için diferansiyel taramalı kalorimetre (DSC) cihazı kullanılmıştır. Bu geçişin sonucu gözle görülür olduğundan dolayı fotoğraflar ile gösterilmiştir.

Son olarak tezin dördüncü bölümünde, florür anyonun tespiti için oktametilkaliks[4]pirolün reseptör, 4-metilumbelliferon ve floreseinin tetrabutilamonyum tuzlarının indikatörler olarak kullanıldığı düşük maliyetli floresans turn-on IDA sensörleri geliştirilmiştir.

Tüm sensörler florüre karşı diğer anyonlara göre hızlı ve seçici duyarlılık gösterirken, 4-metilumbelliferon bazlı IDA sisteminin aynı zamanda florür anyonunun algılanması için görsel bir renk değişimine sahip olduğu ortaya çıkmıştır. Deneysel sonuçlar, floresein bazlı IDA sensörünün, 3.2 nM kadar düşük bir algılama limiti ile florür anyonunun algılanması için kullanılabileceğini ortaya koymuştur. Bu sensörlerin hem asetonitril hem tetrahydrofuran çözücülerde çalışabılmektedir.

Bu sensörlerin karakterizasyonu çeşitli spektroskopik yöntemler ile yapılmıştır (^{1}H-NMR, ^{13}C-NMR).

Reseptör (oktametilkaliks[4]pirol) ile anyonik indikatörler arasındaki bağlanma sabiti belirleme çalışmaları da ^{1}H NMR titrasyonları kullanılarak CD_3CN'de gerçekleştirilmiştir.

Tersine çevirebilirliği incelenmiştir ve bütün İDA sensörleri fluor anyonu bağladıktan sonra lithium katyonu kullanarak asil halıne geri döndüğü tespit edilmiştir.

Turn-ON, Turn-OFF geçişleri ^{1}H-NMR, fluoresans ve UV-Vis analizleri ile takip edilmiştir.

Renk değişimleri fotoğralar ile gösterilmiştir.

1. INTRODUCTION

Supramolecular chemistry is the chemistry of the intermolecular interactions. It is often defined as “the chemistry beyond the molecule”. The study of non-covalent interactions is very important to understand biological processes which are generally the inspiration of supramolecular chemistry.

The goal in supramolecular chemistry is to build blocks that contain moities that may allow a self-assembly based on non-covalent interactions such as host–guest interactions and hydrogen bonding. The reversibility of these interactionsprovides to the resulting materials a responsivness against various stimuli e.g., temperature, pH and so on. This fact makes the supramolecular polymers very attractive as it combines the properties of conventional polymers with the responsivness to stimuli. Pillar[5]arenes, cyclodextrins, calixarene , crown ethers are few examples of currently used molecules as supramolecular host to prepare stimuli responsive materials. The properties of those kind of materials are mostly based on the host guest chemistry. Calix[4]pyrroles exhibit selective anion binding properties in aprotic solvents (e.g. methylene chloride, chloroform and dimethylformamide). They have been used in several applications such as electroactive sensors, anion separating solid supports, molecular containers and nanosensors. However, their utilization and applications in supramolecular polymer chemistry is still rare.

Ion pair receptors have been shown potential in controllable recognition of cations and anions simultaneously, which has made a vital contribution to various research fields. Moreover, molecules that can recognize anions gained a growing interest in areas such as biotechnology and environmental chemistry. They can also be used as phase transfer catalyst, anion selective optical sensors. Apart from that, there are also applications in the field of chromatography. However, weak anion-receptor interactions, especially the interactions between neutral receptors and anions, make the design and synthesis of those kind of receptors difficult. Although, several achievements have been made, ease of design, synthesis, and application of anion based ion-pair recognition is an ongoing challenge.

1.1 Purpose of Thesis

The aim of this thesis is the easy and cost-effective preparation of calix[4]pyrrole based high molecular weight supramolecular polymers and to investigate their properties against various stimuli such as temperature and chemical. The selective anion sensing ability of calix[4]pyrrole skeleton was also particularly investigated. The last part of the thesis focuses on this subject and is about a very simple and cost-effective anion sensing system based on simple calix[4]pyrrole entity which may find utility in the rapid determination of low concentration fluoride anion in organic media.

Each chapter of this thesis has its own introduction, conclusion, and list of references as it corresponds to a scientific article published during this PhD.

2. A THERMORESPONSIVE SUPRAMOLECULAR GEL FROM A HETERODITOPIC CALIX[4]PYRROLE[1]

2.1 Introduction

Supramolecular polymers, integrating the polymer science and supramolecular chemistry, is one of the rapidly developing interdisciplinary research fields. A number of noncovalent interactions (e.g., π-π stacking, host-guest interactions, metal coordination, and hydrogen bonding) have been employed as directional and reversible forces to serve polymeric properties in solution and bulk.[1] This has allowed the production of adaptive materials and bestowed functions such as self- healing, thermo- and stimuli-responsiveness.[2] To date, various supramolecular hosts, including crown ethers [3], calixarenes [4], cyclodextrins [5], cucurbiturils [6], and pillar[5]arenes [7], have been widely used to prepare such materials whose properties can be controlled by pH, temperature and light.

Calix[4]pyrroles (**1**) can bind anions selectively in common aprotic organic solvents (e.g., $CHCl_3$, and CH_3CN).[8] They have been utilized as ion selective optical [9] and electro active sensors, [10] anion extractants,[11] anion separating solid supports, trans-membrane ion transporters, [12] molecular containers, [13] and nanosensors [14] are the examples of the systems that have been developed for various applications to mention but a few. However, their utilization in the supramolecular polymer chemistry is rare. For instance, tetrathiafulvalene- functionalized, [15] bis(dinitrophenyl)-meso-substituted [16] and imidazolium tethered calix[4]pyrroles [17] have been used to obtain supramolecular assemblies. Although, the resulting supramolecular assemblies were found to undergo dynamic guest-dependent structural transformations, these systems exhibited relatively low degree of supramolecular polymerization in solution. These findings prompted us to design easy-to-prepare,

[1] This chapter is based on the paper "A Thermoresponsive Supramolecular Polymer Gel from a Heteroditopic Calix[4]pyrrole" by Sana Amharar, Abdullah Aydoğan, 2018, *Chemical Communication* vol 54, 829-932.

highly soluble heteroditopic calix[4]pyrrole monomers bearing a negatively charged moiety that the tetrapyrrolic macrocycle can bind strongly (Figure 2.1).

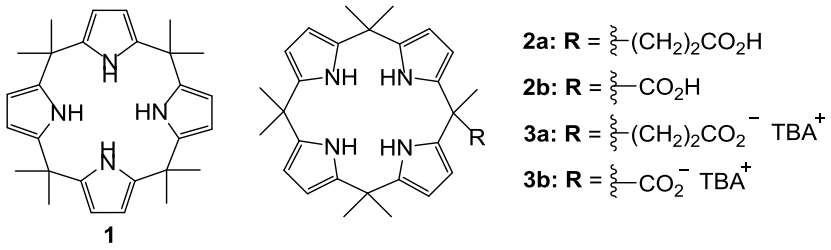

Figure 2.1 : Structures of octamethylcalix[4]pyrrole (**1**), carboxylic acid functionalized calix[4]pyrroles (**2a** and **2b**) and their tetrabutylammonium salts (TBA) (**3a** and **3b**).

Therefore, we decided to prepare carboxylate- functionalized calix[4]pyrroles in the form of their TBA^+ salts (**3**). It is known that if the heteroditopic supramolecular monomer has enough stiffness the formation of intramolecular complexes can be prevented [19]. Hence, the short distance between calix[4]pyrole cores and the carboxylate units of **3a** and **3b** is expected to prevent the intramolecular complexations and allow the formation of supramolecular polymeric assemblies at high concentrations.

2.2 Results and Discussion

Towards these goals, compound **3a** and **3b** were prepared quantitatively via a precipitation reaction from the solutions of **2a** [10] and **2b** [20] in diethyl ether by addition of tetrabutylammonium hydroxide.

X-ray quality crystals of **3b** were obtained by slow diffusion of diethyl ether into a 0.014 M acetonitrile solution of **3b**. The resulting crystal structure confirmed that this heteroditopic calix[4]pyrrole interacts with another macrocycle at low concentrations to self-assemble into dimers in solid state. As shown in Figure 2.2, a carboxylate unit from one molecule of **3b** is hydrogen-bonded to the pyrrole core of the second molecule while this second macrocycle sharing its carboxylate with the first calix[4]pyrrole subunit while attaining a cone conformation.

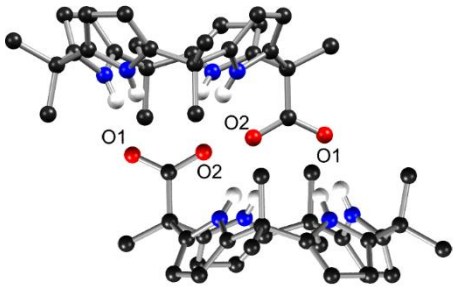

Figure 2.2 : Side view of the supramolecular dimer of **3b**-**3b** in the solid state obtained from a low concentration solution of **3b** in CH_3CN (Hydrogen atoms, TBA^+ and solvent atoms were removed for clarity).

To assess the self-complexation of **3a** and **3b** their ^{1}H-NMR spectra in CD_3CN were also compared with ^{1}H-NMR spectra of their precursors **2a** and **2b** (Figure 2.3).

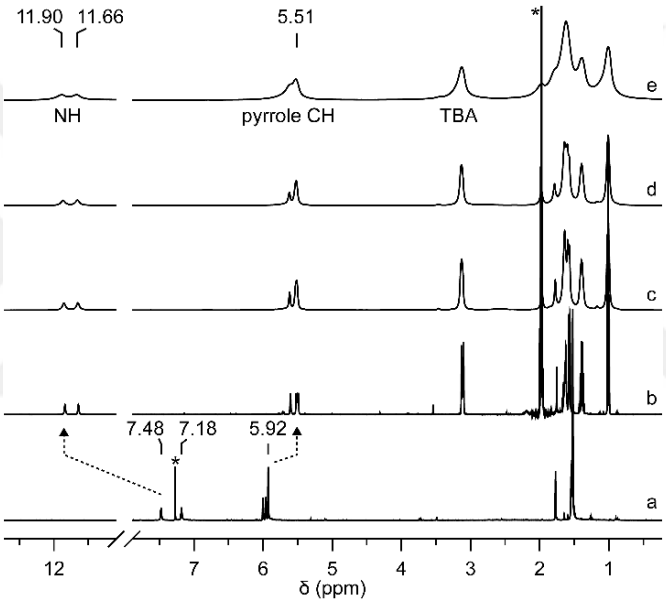

Figure 2.3 : Partial ^{1}H NMR spectra of a) **2b** (0.02 M in $CDCl_3$) and **3b** (in CD_3CN): b) 0.025, c) 0.49, d) 0.75, e) 0.89 M. * denotes the solvent residual peaks

The spectra of initial carboxylic acid-functionalized calix[4]pyrroles and their carboxylate salts differ dramatically. For instance, pyrrole NH proton signals of **2b** were observed at 7.18 and 7.48 ppm as two distinctive peaks (Figure 2.3 a). In the case of **3b** these peaks were found to shift downfield to 11.66 and 11.90 ppm. In contrast, pyrrole CH proton resonances of **2b** gave raise around 5.92 ppm, whereas the corresponding peaks of **3b** resonate around 5.51 ppm. The nature of these lower and upper field peak shifts are typical of what is observed when a calix[4]pyrrole is bound to an anion [23]. Similar to above results, pyrrole NH and CH peaks of **2a** and **3a** were also found to be shifted accordingly (Figure 2.4).

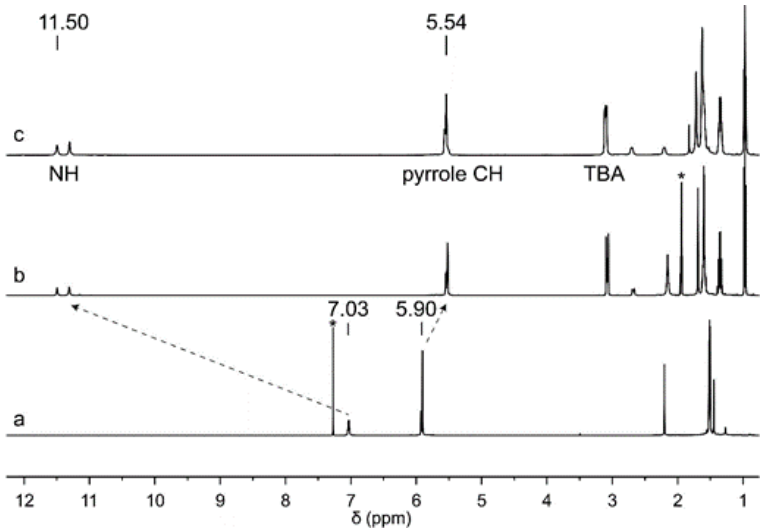

Figure 2.4 : Partial ^{1}H NMR spectra of a) **2a** (0.02 M in $CDCl_3$) and **3a** (in CD_3CN): b) 0.025, c) 0.49, d) 0.75, e) 0.89 M. * denotes the solvent residual peaks

These results clearly show that **3a** and **3b** exhibit intermolecular interactions in solution. The concentration-dependent ^{1}H-NMR analysis provides important insights into the self-assembly behaviours of supramolecular aggregates in solution.[2d, 17, 24]. Although, the calix[4]pyrrole **3b** exhibited a dimer formation in solid state (**3a** was also expected to behave the same as inferred from its ^{1}H NMR spectrum shown in Figure 2.4.b), **3b** and **3a** were expected to self-assemble into higher order supramolecular aggregates at elevated concentrations. This is because the single crystals of **3b** were grown at a very low concentration, which is 0.014 M. It is also known that the formation of long chain supramolecular polymers requires either a large binding constant or high monomer concentrations [25]. Calix[4]pyrroles **3a** and **3b** meet these criteria since the binding constant between calix[4]pyrrole core and acetate anion is large (Ka = $3.5\times10^{5}\pm8.1\times10^{3}$ M^{-1} in CH_3CN) [18] and high concentration solutions can be prepared in CH_3CN as can be judged from Figures. 2.3 and 2.4. In accordance with the above discussions, concentration-dependent ^{1}H-NMR analyses of **3a** and **3b** were carried out in CD_3CN. As shown in Figures 2.3 and 2.4, calix[4]pyrroles **3a** and **3b** were found to behave different as the concentrations of solutions were increased. An inspection of Figure 2.4 reveals no significant peak broadenings when the concentration of **3a** increased from 0.025 to 0.79 M. In contrast, as the concentration of **3b** was increased gradually from 0.025 to 0.89 M, all proton signals of **3b** became significantly broader, indicating the formation of large size supramolecular aggregates when **3b** used as a supramolecular monomer.To analyze further the supramolecular polymers obtained from **3a** and **3b**, viscosity measurements

were carried out in CH_3CN using an Ubbelohde semi-micro dilution viscometer. As depicted in Figure 2.5, double logarithmic plot of specific viscosity (Vs) versus the concentration of **3a** and **3b** exhibited viscosity transitions. The curves belonging to **3a** and **3b** have a slope of 1.02 at low concentration ranges, indicating the existence of dimers with constant sizes.

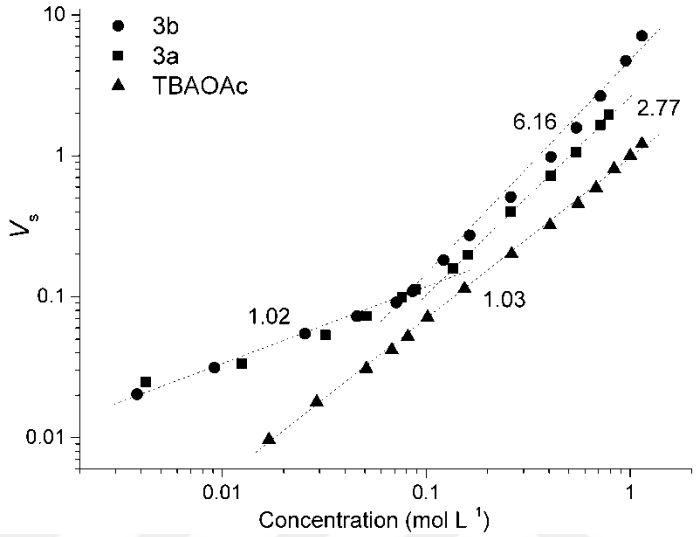

Figure 2.5 : Double-logarithmic plot of specific viscosity changes of **3a**, **3b** and TBAOAc in CH_3CN at 25ºC

As the concentrations of these calix[4]pyrrolesexceed the critical polymerization concentration (CPC = 118 and 79 mM for **3a** and **3b**, respectively), increases in the specific viscosities were observed. For instance, **3b** revealed a slope of 6.16, demonstrating the presence of supramolecular aggregates in which the length of the resulting supramolecular polymer increased with the increment in the monomer concentration. The slope of curve belonging to **3a** was calculated to be 2.77, reflecting the existence of dimers even at high concentration ranges. In contrast to the above data, as a control, viscosity measurements of tetrabutylammonium acetate (TBAOAc) showed a linear relationship, indicating the absence of higher order aggregates at elevated concentrations. The non-linear increment in the viscosities of **3a** and **3b** serve to rule out of two different binding mode scenarios. These include a dimer formation in which two calix[4]pyrrole carboxylates interact with each other at low concentrations and the intermolecular interactions wherein the pyrrole NHs and carboxylate anions are bound to each other to lead the formation of supramolecular polymers at high concentrations (cf. Figure 2.6 and Figure 2.2).

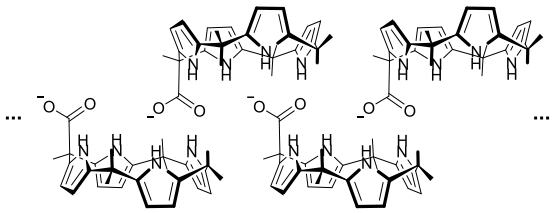

Figure 2.6 : Schematic representation of of the proposed supramolecular polymer formed *via* the self assemblie of **3b** at high concentration.

Furthermore, correlated 2D-NOESY signals were observed between pyrrole-CH and meso-CH_3 protons of **3b** at high concentrations. These findings provide further support for the proposed binding mode change and overhauser effect when the concentration of **3b** was increased (Figure 2.7 and 2.8, ESI†).

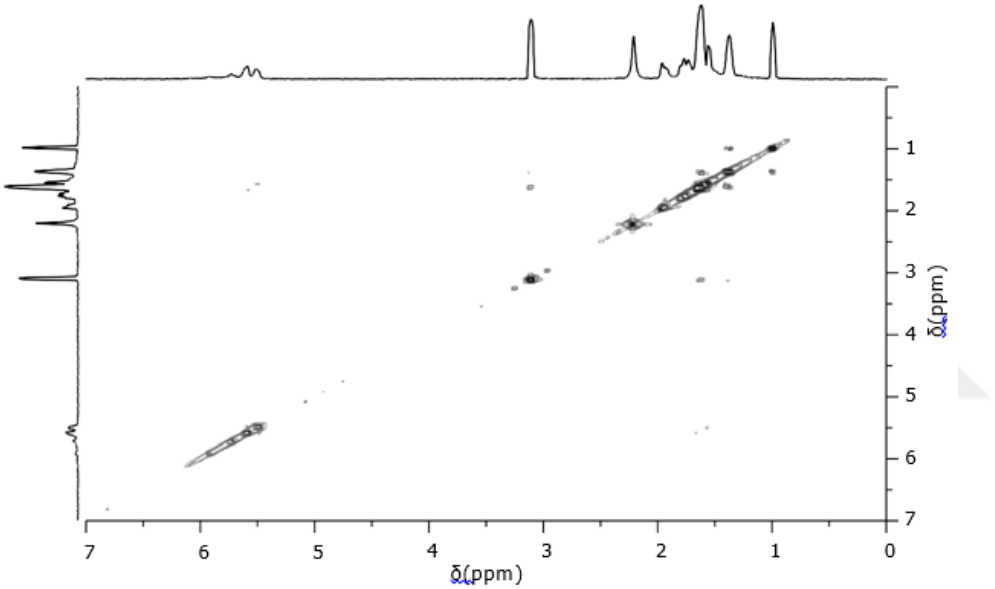

Figure 2.7 : Partial NOESY NMR spectrum of **3b** (0.02M) recorded in CD_3CN.

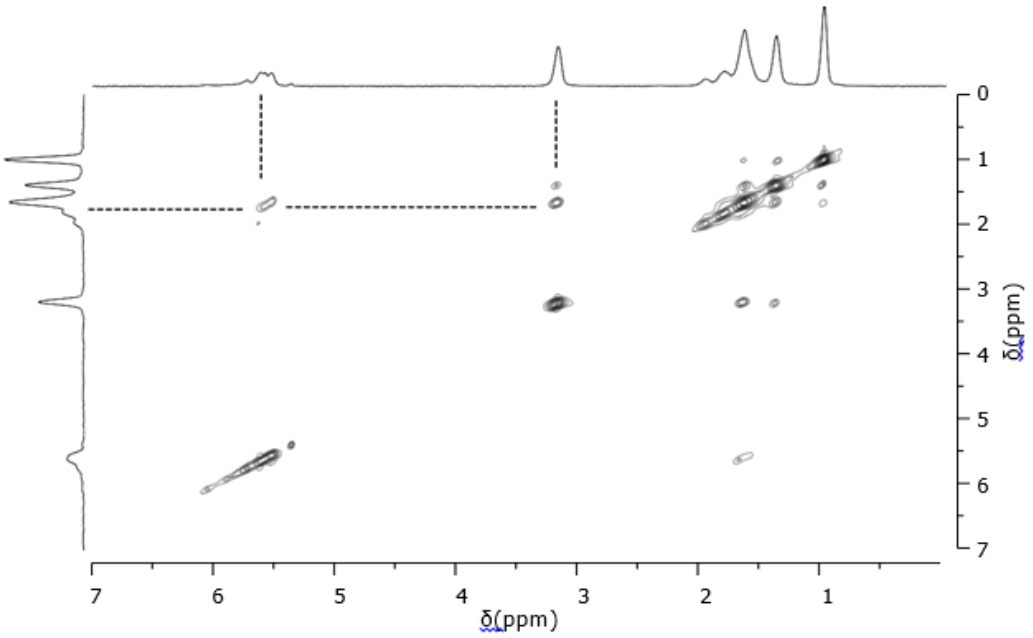

Figure 2.8 : Partial NOESY NMR spectrum of **3b** (0.89M) recorded in CD_3CN.

Diffusion ordered ^{1}H-NMR spectroscopy (DOSY) can be used to compare the sizes of supramolecular polymers quantitatively by comparison of their diffusion coefficients [25,26]. Therefore, DOSY experiments were performed to investigate the self-aggregation performances of **3a** and **3b**. In accord with the design expectations, as the monomer concentration of **3b** increased from 0.02 to 0.75 M, the measured weight average diffusion coefficient (D) of aggregates decreased from 8.81×10^{-10} to 0.79×10^{-10} m^2s^{-1}(Figures 2.9 and 2.10) corresponding to a 91% nonlinear change. However, D of residual solvent was found to exhibit a 78% linear decrease.

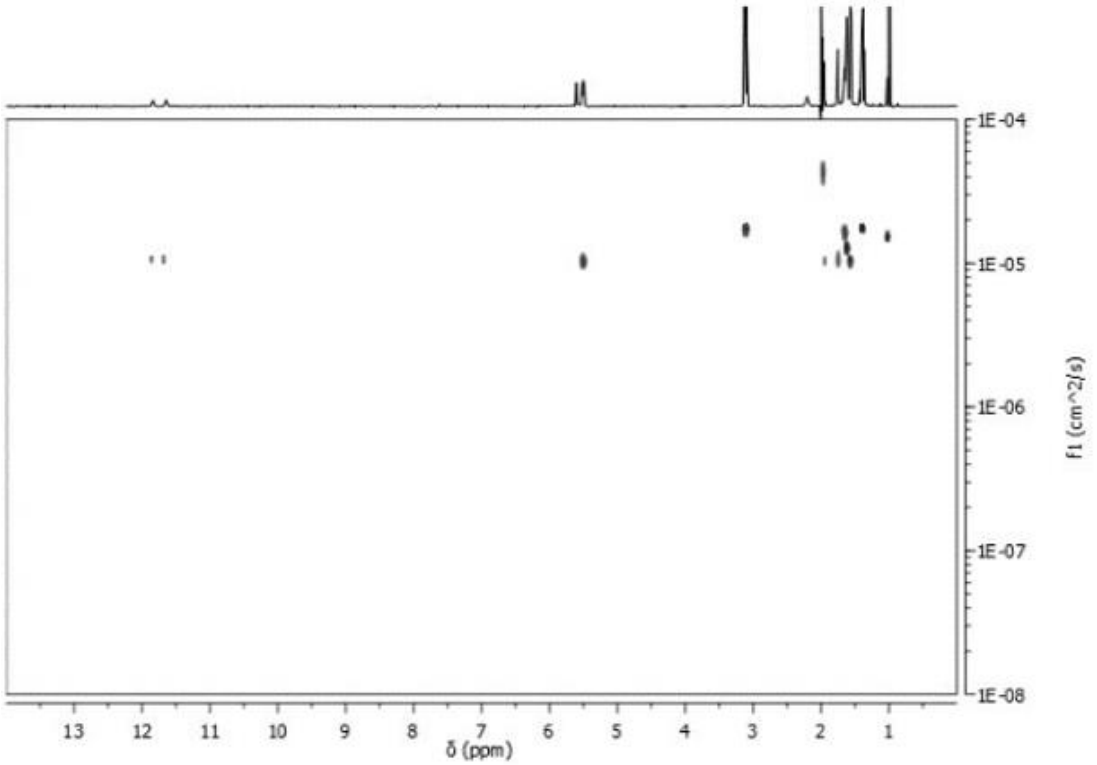

Figure 2.9 : DOSY NMR spectrum of **3b** (0.02M) recorded in CD_3CN at 25ºC.

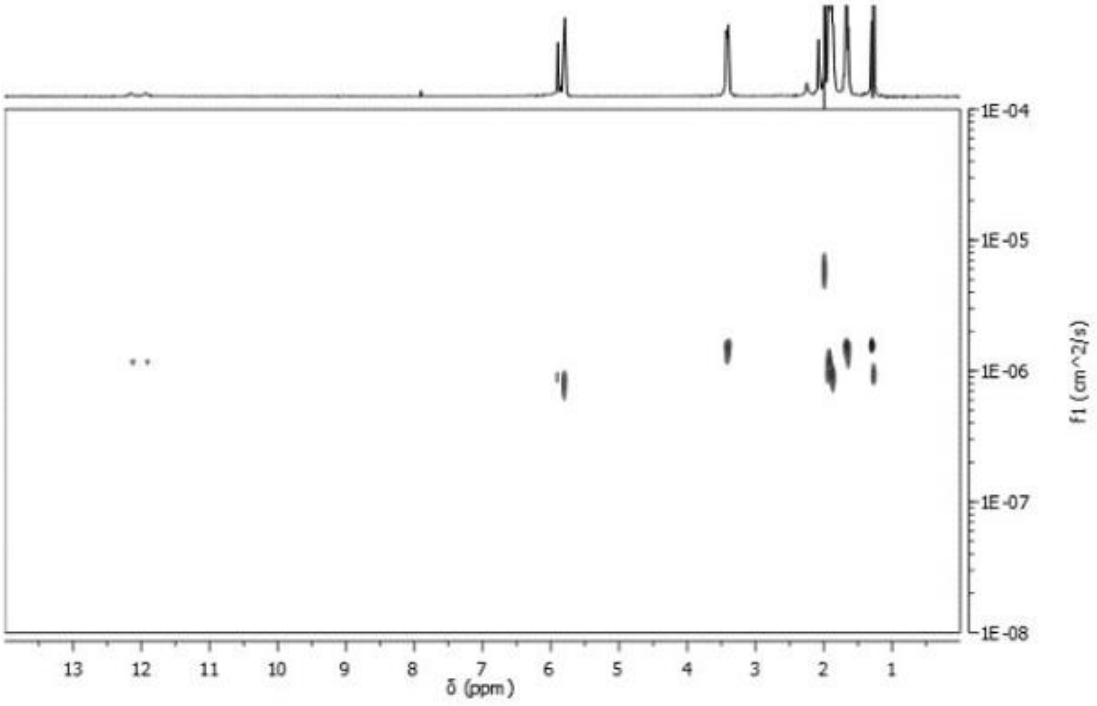

Figure 2.10 : DOSY NMR spectrum of **3b** (0.75M) recorded in CD_3CN at 25ºC.

This result was thought to indicate the supramolecular polymerization of monomer **3b** based on the fact that a high degree of polymerization is necessary to observe a sharp decrease in the diffusion coefficient.[24d, 27] In the case of **3a** these diffusion

coefficients were found to be 9.51×10^{-10} to 2.12×10^{-10} m^2s^{-1} under the same concentration margins. Furthermore, the size of supramolecular dimer **3b-3b** was measured as 14.961 Å from its solid state and compared with its hydrodynamic diameter which was calculated as 13.45 Å by using Stokes-Einstein equation, diffusion coefficient and the viscosity of 0.02 M solution. Based on the above results, it was concluded that **3b** exhibits a distinguishable performance compare to monomer **3a**. This was thought to be the existence of stable supramolecular dimers at all concentration ranges of **3a**. Additionally, the number of methylene units between carboxylate unit of **3a** (two methylene units) and its calix[4]pyrrole core is very close to another calix[4]pyrrole structure with three methylene spacers which was reported earlier and found to exhibit stable supramolecular dimers both in solution and solid state.[28] Additionally, while a 1.2 M CH_3CN solution of **3b** can be prepared, the highest concentrated solution that can be obtained by using **3a** was found to be 0.79 M. Furthermore, tetramethyl- and tetraethylamonium salts of **3a** and **3b** were not found to have good solubilities in CH_3CN when the effect of these counter cations was taken into account. Since **3b** has better solubility and attains longer supramolecular aggregates, rod-like fibers were also drawn successfully from a high concentrated solution of **3b**. Scanning electron microscopy (SEM) image of fiber is shown in Figure 2.11 and revealed a fiber with 10 μm diameter, providing direct evidence for the formation of a supramolecular polymer with high molecular weight.[24b, 24c]

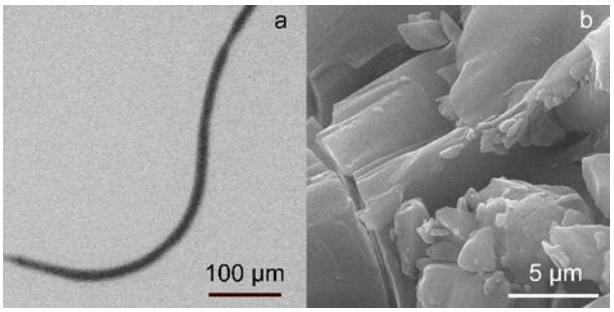

Figure 2.11 : SEM micrographe of gold-coated a) fiber drawn from a high-concentration CH_3CN solution of **3b**, and b) supramolecular polymer gel obtained *via* freeze drying of 0.9 M CH_3CN solution of **3b**.

Compound **3b** consists of a calix[4]pyrrole core and a tethered carboxylate unit. Hence, the degree of polymerization ($DP \approx (K_aC)^{1/2}$) could be estimated using the isodesmic model in conjunction with the affinity constant between the parent system **1** and acetate anion ($Ka = 3.5\times10^5\pm8.1\times10^3$ M^{-1}) [25, 29]. The resulting value, which corresponds to the average number of subunits in the supramolecular polymer, was

estimated to be 558±6 for **3b** at a concentration of 0.89 M in CH_3CN at 25 °C (Table 2.1).

Table 2.1 : Estimatedvaluesof DPat different concentrations of **3b**.

3b (mol L-1)	DP_{max}
0.25	296±3
0.49	414±4
0.75	512±5
0.89	558±6
1.2	648±7

Gelation and thermoresponsive behaviour of **3b** were also investigated. As shown in Figure 2.12b, after heating to 50 °C, the supramolecular polymer gel formed by 0.9 M **3b** was dissociated into a solution immediately. Reformation of the supramolecular polymer gel was achieved by cooling to 20 °C and standing for 5 min (Figure 2.12a).

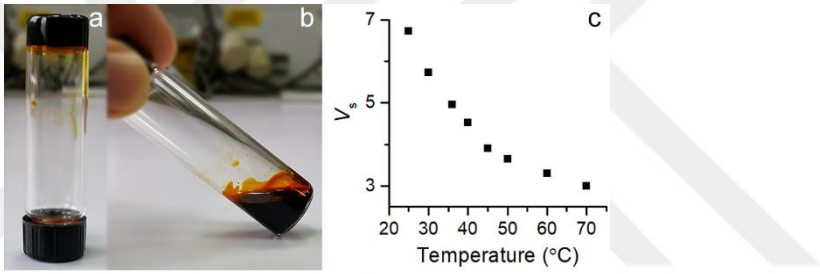

Figure 2.12 : Inversed-vial test of supramolecular polymer obtained from a 0.9 M CH_3CN solution of **3b** at (a) 20 °C, (b) 50 °C, and (c) temperature dependent viscosity change of the same solution.

SEM image of the freeze-dried gel sample exhibited a paraffin like network structure (Figure 2.11 b). Variable temperature viscosity measurements were also performed to support the thermoresponsive behaviour of supramolecular polymer formed by **3b**. Figure 2.7c shows the specific viscosity change of a 0.9 M CH_3CN solution of **3b** upon change in the temperature. While the specific viscosity of aforementioned solution was 6.73 at 25 °C it was found to be decreased sharply to 3.00 when the temperature was increased to 70 °C. These findings reflect the presence of high molecular weight supramolecular aggregates at low temperatures and the dynamic nature of non-covalent interactions between calix[4]pyrrole units. We also examined other solvents (e.g., $CHCl_3$ and CH_2Cl_2) to induce gelation of **3b**. While supramolecular polymerization of **3b** was observed, high concentrated solutions of **3b** could not be obtained for further gelation.

2.3 Conclusion

In conclusion, linear supramolecular polymers can easily be formed driven by the hydrogen bonding interactions between calix[4]pyrrole NHs and tethered carboxylate functional groups. By combination of X-ray, ^{1}H-, NOESY, DOSY NMR analyses, and viscosity measurements revealed that while **3a** and **3b** forms dimers at low concentrations, when the concentration exceeds the CPC **3b** was found to form linear supramolecular polymers with a high degree of polymerization. Additionally, rod-like fibers were also drawn successfully from a high concentrated solution of **3b**, thus providing a direct evidence for the formation of supramolecular polymers with high molecular weights. Considering the ease of synthesis and the thermoresponsive behaviour of the resultant supramolecular polymer gel, the present study illustrates the first example of a high performance supramolecular polymer and its gelation based on the anion recognition chemistry of calix[4]pyrroles.

2.4 Experimental Section

2.4.1 General information

All solvents were dried before use according to standard procedures. Unless specifically indicated, all other chemicals and reagents used in this study were purchased from commercial sources and used as received. ^{1}H, ^{13}C, DOESY and NOESY NMR spectra were recorded on an Agilent VNMRS 500 spectrometer using TMS as an internal reference. Mass spectra were measured on a Thermo Scientific TSQ Quantum GC and Micromass Autospec Ultima. Viscosity measurements were carried out with an Ubbelohde micro dilution viscometer (Shanghai Liangjing Glass Instrument Factory, 0.40 mm inner diameter) at 293 K in chloroform. X-ray crystallographic analyses were carried out on either a Bruker D8 Venture advance diffractometer using Cu Kα radiation with $\lambda = 1.542$ Å. Further details of the structures and their refinement is given in a later section. Compounds **2a** and **2b** were synthesized according to previously reported literature procedures.

2.4.2 Synthesis

2.4.2.1 Compound 3a

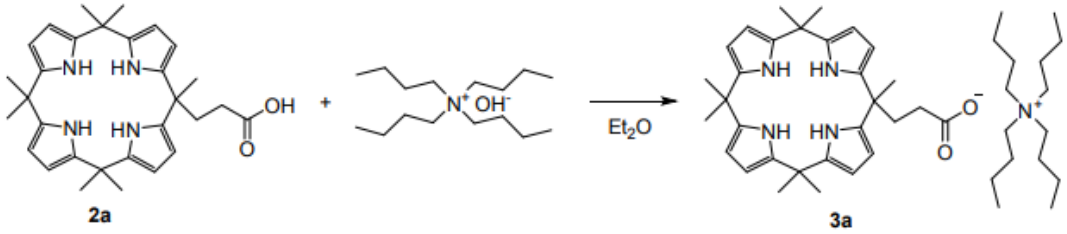

2a 3a

To a solution of **2a** (800 mg, 1.03 mmol) dissolved in 250 mL diethyl ether, methanol solution tetrabutylammonium hydroxide (100 mM, 20 mL) was added dropwise. The reaction mixture was stirred at room temperature for 1h. The resulting precipitate was filtered and washed with excess diethyl ether followed by drying in vacuo afforded **3a** as a white solid (1.15 g, 96%). M.p.: decomposes at 223 °C. ^{1}H NMR (500 MHz, CD3CN, 25 °C): δ = 0.97 (t, J=7.4 Hz, 12H, –CH3), 1.35 (m, 8H, –CH2–), 1.60 (br m, 21H, meso–CH3), 1.69 (br m, 10H, –CH2–), 2.68 (m, 2H, –CH2–), 3.04-3.11 (m, 8H, –CH2–), 5.52 (m, 8H, pyrrole–CH), 11.31 (br s, 2H, NH), 11.50 (br s, 2H, NH). 13C NMR (126 MHz, CD3CN): δ = 181.02, 140.01, 100.61, 58.35, 37.82, 37.12, 34.39, 28.56, 27.09, 23.33, 19.36, 12.80. Elemental analysis: calculated for $C_{46}H_{73}N_5O_2$: C 75.88, H 10.11, N 9.62; found C 75.05, H 9.94, N 9.53.

2.4.2.2 Compound 3b

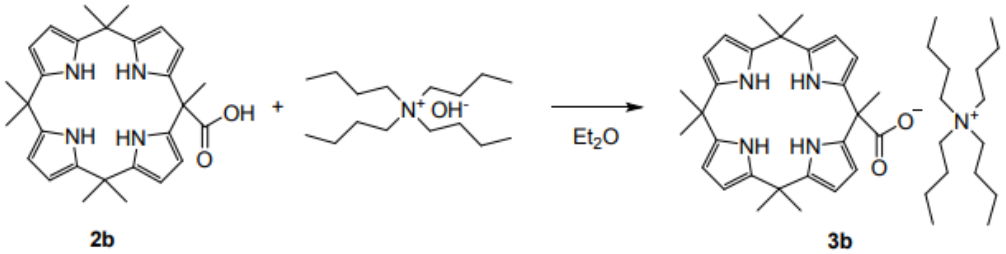

2b 3b

This compound was prepared from **2b** (800 mg, 1.74 mmol) using the same procedure that was used to produce **3b**. The product was a white solid (1.18 g, 97%). M.p.: decomposes at 200 °C. ^{1}H NMR (500 MHz, CD_3CN, 25 °C): δ = 0.97 (t, J=7.3 Hz, 12H, –CH3), 1.36 (m, 8H, –CH2–), l.54 (m, 8H, –CH2–), 1.57-1.63 (br m, 18H, meso–CH3), 1.72 (br s, 3H, meso–CH3), 3.06-3.10 (m, 8H, –CH2–), 5.45-5.57(m, 8H, pyrrole–CH), 11.61 (br s, 2H, NH), 11.80 (br s, 2H, NH). 13C NMR (126 MHz, CD3CN): δ = 181.33, 140.95, 140.41, 139.85, 138.97, 100.24, 58.38, 34.30, 28.58,

26.98, 24.54, 23.33, 19.34, 12.81. Elemental analysis: calculated for $C_{44}H_{69}N_5O_2$: C 75.49, H 9.94, N 10.00; found C 75.12, H 9.81, N 9.91.

3. AN ION PAIR RECOGNITION BASED SUPRAMOLECULAR POLYMER SHOWING RAPID AND REVERSIBLE SOL-GEL TRANSITION THROUGH VAN DER WAALS INTERACTION[2]

3.1 Introduction

Ion pair recognition is a well-established research field whose impact comprises important applications, including sensors,[30] selective salt extraction [31,32] transmembrane transport,[33] information processing,[34] and metal organic frameworks.[35] Among the several classes of ion pair receptors (e.g., pyrrole, imidazole, and macrocycles) [36] calix[4]pyrroles draw particular attention because of their versatility in binding mode which is used as a criterion to categorize ion pair host systems.[37] After discovery of the ion pair recognition ability in solid state [38] and solution [39], several type of ca-lix[4]pyrrole systems (e.g., strapped-, fused- and bis-calix[4]pyrroles) have been reported to sense or extract various ions as well as binding mode and 2[rotaxane] engineer-ing.[40-42] Owing to the positive allosteric effect[36] rationally designed calix[4]pyrrole architectures, wherein conformational changes play a critical role in the establishment of host-separated binding mode,[43] have found further applications in anion recognition induced ion pair receptors [38,39], especially in the case of alkylammonium salts.[44]

These advancements prompted us to design a highly soluble heteroditopic calix[4]pyrrole monomer functionalized with a negatively charged domain that can interact with the anion-bound calix[4]pyrrole throughcation–πinteractions. Van der Waals interactions also have very critical role in the formation of self-assembled structures.[45] Hence, synthetic self-assembled supramolecular polymers that are formed through ion pair recognition of this AB type monomer, could be crosslinked *via* van der Waals interactions of alkyl chains which would allow us to control the

[2] This chapter is based on the paper "Ion pair recognition based supramolecular polymer showing rapid and reversible Sol-Gel transition through Van deer Waals's interaction" by Sana Amharar, Armağan Atsay, Abdullah Aydoğan.2020, *ACS Applied Polymer Materiel*, 2, 5371-5376.

crosslinking of the supramolecular polymer. The parent macrocycle **1** is known to bind acetate anion well in organic media.[46] Therefore, a carboxylate functional calix[4]pyrrole bearing cetyltrimethylammonium (CTA) as a counter cation was prepared to form an ion pair recognition based supramolecular polymer that can exhibit rapid and reversible sol-gel transition through van der Waals interactions.

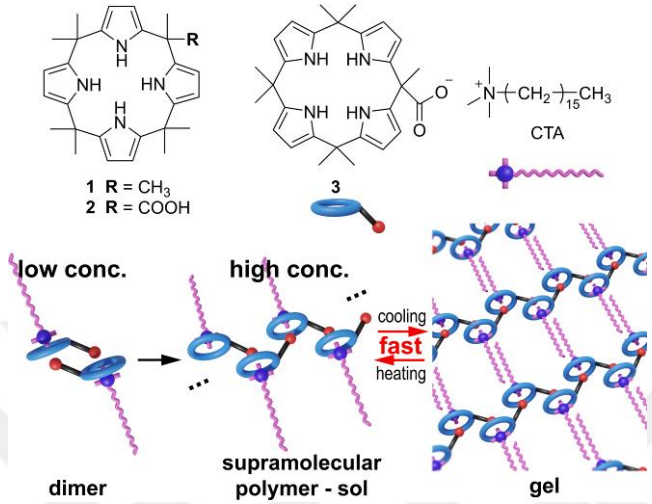

Figure 3.1 : Structures of octamethylcalix[4]pyrrole (**1**), its carboxylic acid (**2**) and carboxylate (**3**) derivatives. Cartoon representation of rapid and reversible sol-gel transition shown by the supramolecular polymer obtained from **3**

During a supramolecular polymer formation, the existence of intramolecular complexes can be disregarded if the supramolecular monomer has enough stiffness, which prevents guest unit curling around to complex with the host intramolecularly.[47] The calix[4]pyrrole core of **3** also prevents intramolecular complexation because of the short distance between calix[4]pyrrole and carboxylate units based on the conclusions of our previous report.[48] Thus, **3** is expected to form polymeric assemblies at elevated concentrations.

3.2 Result and Discussion

With these in mind, treatment of carboxylic acid precursor **2** [49] with cetyltrimethy-lammonium hydroxide (CTAOH) in diethyl ether allowed us to obtain **3** quantitatively as a pale-yellow solid.The self-complexation behavior of **3** was investigated by utilizing NMR spectroscopy. For that purpose, the ^{1}H NMR spectrum of **3** was compared with that of **2** and CTOH. A substantial difference was observed when the spectra of initial carboxylic-acid-functionalized calix[4]pyrrole **2** and its carboxylate

salt **3** were compared. The first set of peak shifts in Figure 3.2 is related to the host-guest interaction of calix[4]pyrrole and tethered carboxylate unit.

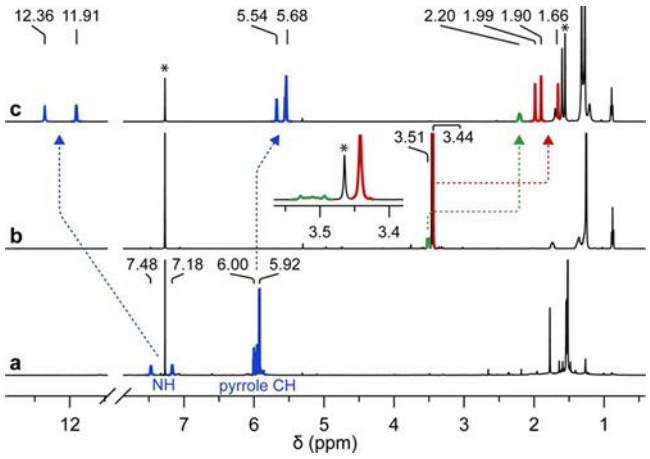

Figure 3.2 : ^{1}H NMR spectra of (a) **2**, (b) CTAOH, and (c) **3** recorded in CDC_3. The asterisk (*) denotes solvent and H_2O residual peaks.

The first set of peak shifts in Figure 3.2 is related to the host-guest interaction of calix[4]pyrrole and tethered carboxylate unit. Two distinctive pyrrole NH proton signals at 7.18 and 7.48 ppm were observed in the spectrum of carboxylic acid **2**, whereas the corresponding peaks were found to resonate at 11.91 and 12.36 ppm. In contrast to these downfield shifts, pyrrole CH proton resonances of **3** appeared around 5.68 ppm, whereas the corresponding peaks appeared around 5.96 ppm in the case of **2**. These lower and upper field peak shifts are typical of what is observed when a calix[4]-pyrrole is bound to an anion, indicating the host−guestinteraction between the calix[4]pyrrole core and the carboxylate unit of **3**.[40] It is well-known that when calix[4]pyrroles were bound to an anion, they adopt a cone-like conformation such that the four NH protons can hydrogen bond to the anion. Meanwhile, the anion-bound calix[4]pyrrole forms a "cup-like" π electron cloud by means of oriented pyrrole rings.[50] Thus, the second set of peak shifts of Figure 3.2 is related to the catio–π interaction between the π electron cloud of the carboxylatebound cone of **3** and the ammonium head of CTA. In this instance, whereas methylene protons connected to the nitrogen atom of CTAOH exhibited a resonance signal at 3.51 ppm, they were found to shift to 2.20 ppm in the case of **3**. Similarly, methyl protons connected to the same nitrogen atom showed upfield shifts. Initially, they were observed at 3.44 ppm as a single peak (Figure 3.3b), with three distinctive singlet peaks detected at 1.99, 1.90, and 1.66 ppm in the case of **3** (Figure 3.3c). In addition to the chemical shifts of

3 in the ^{1}H NMR spectrum, a cation−π interaction was also monitored using 2D NMR analysis (Figure 3.3).

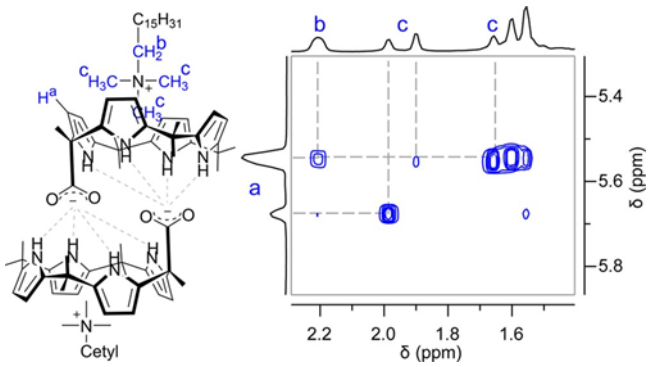

Figure 3.3 : Self-assembled structure and partial ROESY NMR spectrum of **3** recorded in $CDCl_3$.

The correlation signals between pyrrole CH protons and ammonium protons in the ROESY NMR spectrum clearly indicate the cation−π interaction between carboxylate-bound **3** and the ammonium unit of CTA. **3** and similar heteroditopic calix[4]pyrrole structures were found to interact with another macrocycle to self-assemble into dimers via tethered carboxylate−calix[4]pyrrole interactions in the solid state and in solution at low concentrations.[48,51] As illustrated in Figure 3.3, carboxylate units of two different molecules of **3** form hydrogen bonding with pyrrole units of macrocycles while attaining cone conformations. Meanwhile, ammonium units of CTA interact with the electron cloud of cone-shaped macrocycles. As a result of these interactions, **3** forms a rod-like complex structure at low concentrations through host-separated ion pair recognition. Self-assembly behavior of supramolecular aggregates in solution can be assessed using concentration-dependent ^{1}H NMR analyses.[52-54] Although **3** was found to form dimers in solution at low concentrations, it was anticipated to give high molecular weight supramolecular polymers at elevated concentrations. To confirm this expectation, variable concentration ^{1}H NMR analysis of **3** was carried out in $CDCl_3$. As shown in Figure 3.4a−e, all of the resonance signals belonging to **3** broadened significantly as the concentration of solution increased gradually from 0.01 to 0.56 M.

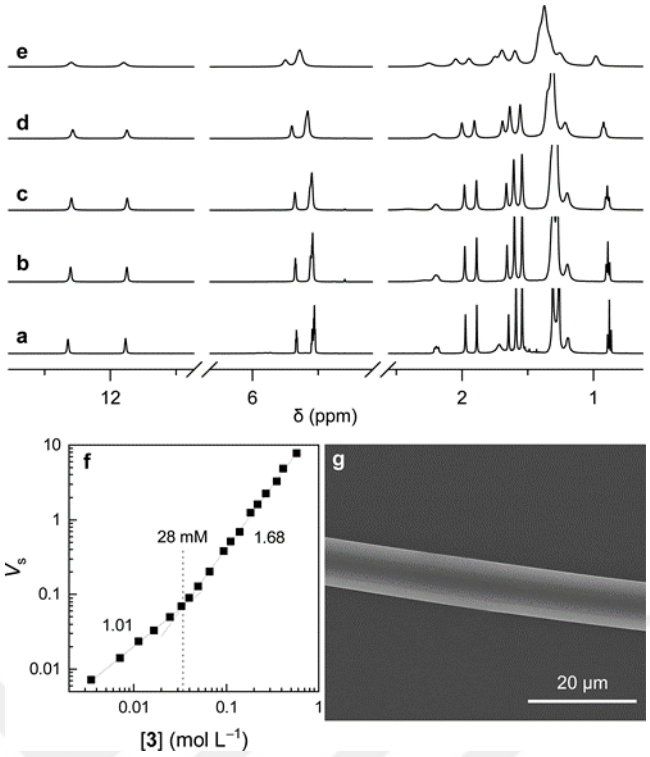

Figure 3.4 : ^{1}H NMR spectra of 3 recorded in $CDCl_3$: (a) 0.01 (b) 0.02, (c) 0.16, (d) 0.30, and (e) 0.56 M. (f) Double logarithmic plot of specific viscosity versus concentration of **3** in $CHCl_3$ at 25 °C. (g) Scanning electron micrograph of a gold-coated fiber drawn from ahighly concentrated solution of **3** in $CHCl_3$.

These peak broadenings were taken as evidence for the formation of supramolecular polymers with a high degree of polymerization [48,45]. In many cases, some chemical shift changes are observed as the supramolecular polymers develop in solution. In the case of **3**, at least pyrrole NH resonance signals are expected to shift downfield at higher concentrations. However, they were found to resonate around 12.3 and 11.9 ppm at all concentration ranges. This result reflects the fact that molecules of **3** that do not participate to the supramolecular polymer chains retain their dimer structure in which pyrrole NHs are bound to carboxylate units. Hence, the chemical shifts of pyrrole NH protons remain unchanged. Sizes of supramolecular polymers can be compared quantitatively using two-dimensional diffusion-ordered NMR spectroscopy (DOSY). Therefore, we performed DOSY experiments to investigate the supramolecular polymerization performance of **3**. In accordance with the above results, as the concentration of **3** increased from 29 to 610 mM, the measured weight-average diffusion coefficient of aggregates decreased considerably from 3.96×10^{-10} to 1.22×10^{-10} m^2 s^{-1}. (Figure 3.5 and 3.6)

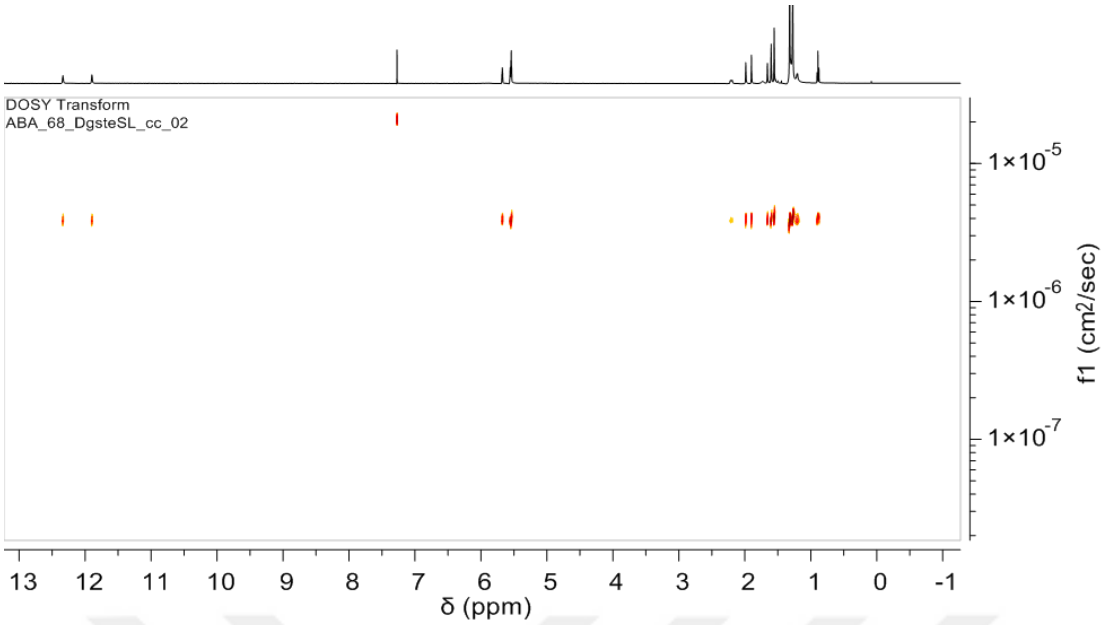

Figure 3.5 : DOSY NMR spectrum of **3** (29 mM) recorded in $CHCl_3$.

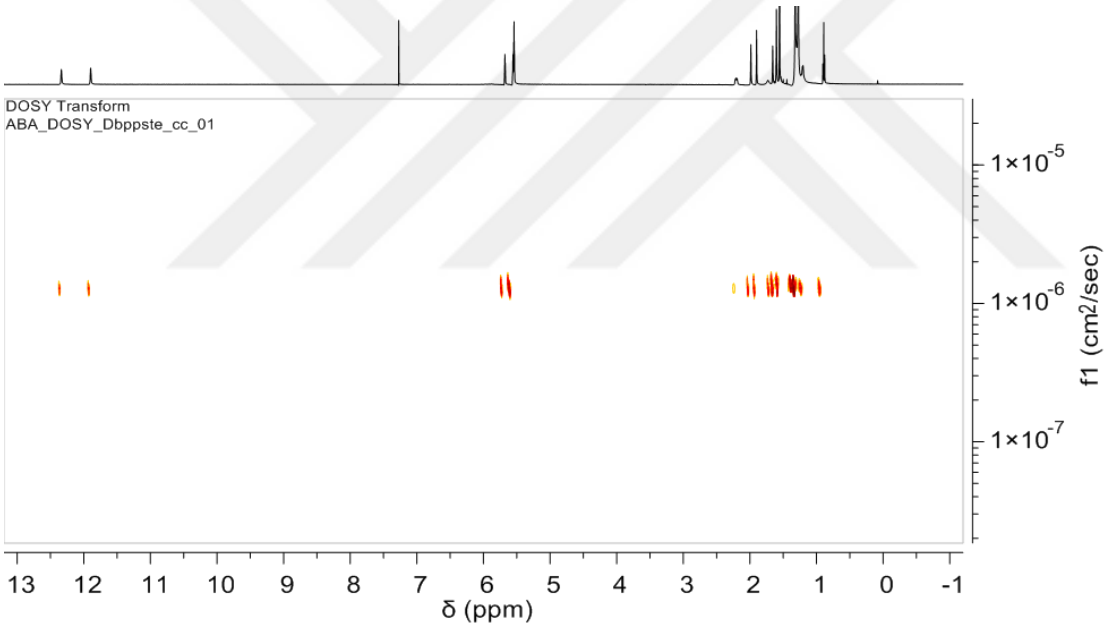

Figure 3.6 : DOSY NMR of **3** (610mM) recorded in $CHCl_3$.

This result was thought to reflect the formation of high molecular weight supramolecular polymers based on the fact that a sharp decrease in the diffusion coefficient is an indication of a high degree of polymerization [56]. To verify that the above NMR signatures correspond to a supramolecular polymerization, concentration-driven specific viscosity measurements were also undertaken. As shown in Figure 3.4f, the double-logarithmic plot of specific viscosity versus concentration exhibits an initial slope (1.01) consistent with assemblies of constant size that changes to a value (1.68) indicative of a linear polymer. The viscosity transition occurs at 28 mM, and on

the basis of prior supramolecular polymerization reports, it is assigned to the critical polymerization concentration. The observation of such viscosity transition is taken as evidence of concentration-driven polymerization of **3** in solution while transforming its binding mode from a dimer to intermolecular interactions wherein the pyrrole NHs and carboxylate anions are bound to each other to lead to the formation of supramolecular polymers at high concentrations (Figure 3.1) [48]. The existence of correlated 2D-NOESY signals at high concentrations between meso-CH_3 and pyrrole ring protons of **3** was thought as further support for such a binding mode change. (Figure 3.7)

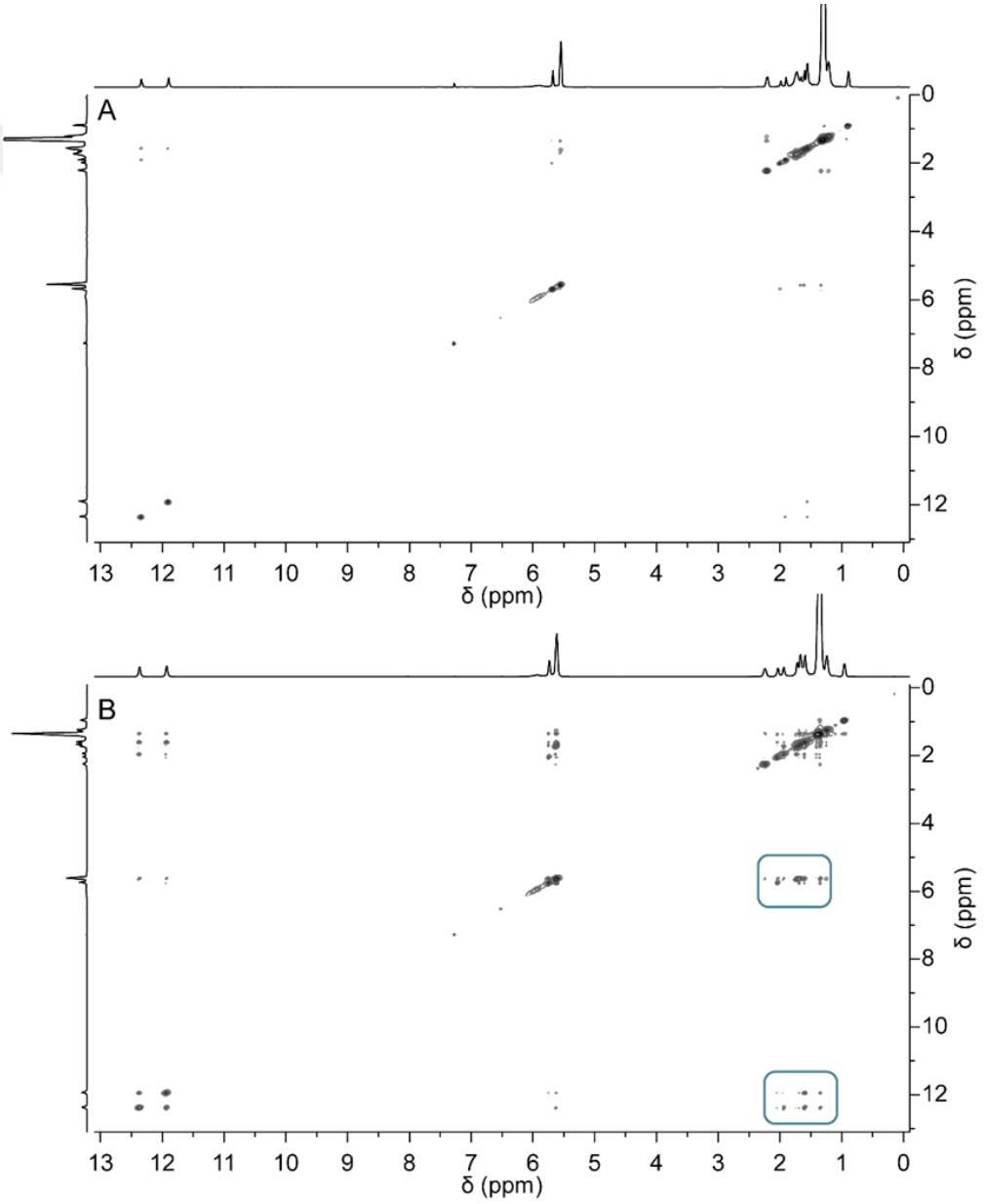

Figure 3.7 : NOESY NMR spectra of **3** recorded in $CDCl_3$ at (A) 29 and (B) 610 mM concentrations.

Another direct evidence for the formation of the supramolecular polymers with high molecular weight came from scanning electron microscopy (SEM) analysis of fibers drawn from a highly concentrated solution of **3** at room temperature. The SEM image of a rod-like fiber is shown in Figure 3.4g and revealed a fiber with a diameter of approximately 8 μm. As **3** can form linear supramolecular polymers through host−guest complexation between calix[4]- pyrroles and tethered carboxylate units, the degree of polymerization (DP ≈ $(KaC)^{1/2}$) could be estimated using the isodesmic model based on the affinity constant between the model system **1** and acetate anion (as CTA salt). The binding constant was determined to be $K_a = 2.1 \times 10^3$ M^{-1} in $CHCl_3$, which is stronger than the corresponding tetrabutylammonium guest.[57] Using this binding constant, the average number of monomers in the supramolecular polymer was estimated to be approximately 30 for **3** at a concentration of 0.51 M in $CHCl_3$. The estimated DP in this manner corresponds to a ∼24 kDa number-average molecular weight. One may wonder whether the supramolecular polymerization of **3** could be achieved in other solvents in which calix[4]pyrroles are commonly utilized for anion recognition. To assess this, the solubility and complexation behavior of **3** was also examined in various organic solvents such as CH_2Cl_2, DMSO, and CH_3CN. During these trials, **3** was found to be highly soluble in CH_2Cl_2 and behave similar to what was observed in $CHCl_3$ in terms of complexation. Pyrrole-NH and −CH resonance signals and CTA-related chemical shifts belonging to **3** were observed in the same region of the ^{1}H NMR spectrum in CD_2Cl_2. Although **3** is not soluble in CH_3CN, it was found to have a slight solubility in DMSO. These findings led us to conclude that supramolecular polymerization of **3** could be achieved in relatively nonpolar solvents. CTA is a direct part of this supramolecular polymer via cation−π interactions (Ka = 1.81×10^3 M^{-1} in $CHCl_3$,). Thus, the long alkyl chains of CTA could exhibit additional hydrophobic interactions requiring relatively low activation energy to be broken, which would allow the supramolecular polymer to show a rapid sol−gel transition depending on the temperature. To test this hypothesis, we first prepared a 0.51 M solution of **3** in $CHCl_3$. As expected, cooling the supramolecular polymer solution of **3** in a vial to 4 °C led to the formation of a self-standing supramolecular gel in 2.5 min (Figure 3.8a), which was anticipated to be formed via hydrophobic interactions between cetyl groups of CTA. As shown in Figure 3.8b, grabbing the vial containing the supramolecular gel at 4 °C and heating in hand allows the restoration of supramolecular polymer solution in 1 min. Thus, the reversible rapid sol−gel transition

induced by temperature could be achieved. The strong correlation signals observed in ROESY and NOESY NMR spectra between the alkyl chain protons of 0.51 M **3** were also considered as additional evidence for thesehydrophobic interactions

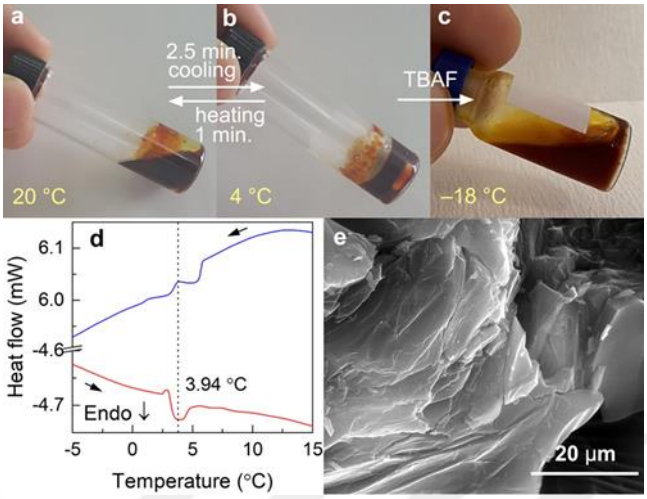

Figure 3.8 : Reversible rapid sol−gel transition of supramolecular polymer obtained from a 0.51 M $CHCl_3$ solution of **3** at (a) 20 °C, (b) 4 °C, and (c) image of sol at -18 °C obtained after addition of equimolar TBAF. (d) Differential scanning calorimetry thermogram of the same concentrated solution and (e) SEM image of supramolecular polymer gel after freeze-drying.

Differential scanning calorimetry (DSC) was also used to monitor sol−gel transition behavior of **3**. For that purpose, a 0.51 M $CHCl_3$ solution of **3** was heated from -5 to 15 °C. As shown in Figure 3.7d, the endothermic transition at 3.94 °C is attributed to the loss of interactions between the long alkyl chains of cetyl groups, as already observed macroscopically around 4 °C. During the cooling cycle, an exothermic transition was observed at the same temperature, corresponding to the establishment of hydrophobic interactions. Thus, the reversibility of the sol−gel transition (ΔH = 0.39 J/g) of the supramolecular polymer obtained from **3** was demonstrated using DSC. When the concentration of **3** was decreased to 0.4 M, the above transitions were observed around -2 °C, indicating the concentration dependence of the sol−gel transition. The freeze-dried gel of **3** was also examined by SEM analysis, which shows a wrinkled, flaky morphology that suggests paraffin-like self-assembly and aggregation of **3** (Figure 3.8e). The effect of a competing anion was also investigated to show the necessity of supramolecular polymer formation for **3** to exhibit rapid sol−gel transition behavior. It is well-known that the calix[4]pyrrole core of **3** binds fluoride stronger than a carboxylate anion.[46,58,60] As the self-assembled structure of **3** is established through host−guest interactions between calix[4]- pyrrole and

tethered carboxylate units, addition of fluoride as a competing anion was expected to decrease the chain length of the supramolecular polymer. The hydrophobic interactions of cetyl units thus will no longer be effective to trigger gelation of shorter supramolecular polymer chains at low temperatures. To test this hypothesis, a 53 mM $CDCl_3$ solution of **3** was titrated with increasing equivalents of tetrabutylammonium fluoride (TBAF). ^{1}H NMR spectra of the resulting mixtures (Figure 3.9) revealed that the calix[4]pyrrole core of **3** not only interacts with a fluoride anion but also keeps complexation with the CTA cation, as inferred from the additional pyrrole NH resonance signals at 13.13 ppm and the chemical shifts of pyrrole CH and ammonium $-CH_3$ protons at upper fields compared to their free congeners **2** and CTAOH.

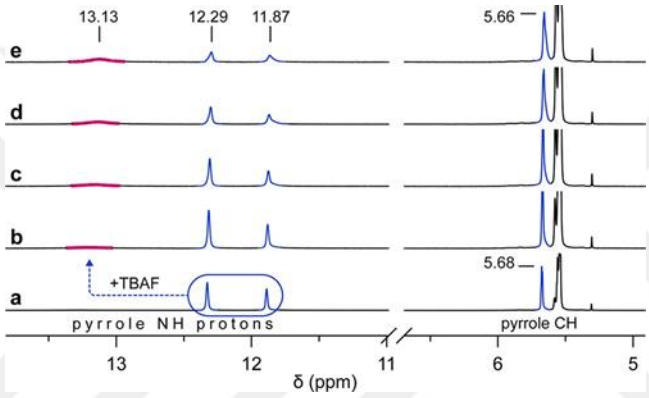

Figure 3.9 : Partial ^{1}H NMR spectra of **3**recorded in $CDCl_3$ aftermaddition of (a) 0.2, (b) 0.4, (c) 0.6, (d) 0.8, and (e) 1.0 equiv of tetrabutylammonium fluoride as a competing anion.

The integration ratio of pyrrole NH protons at 13.13 and 12.29−11.87 ppm was used to calculate the relative proportions of fluoride and carboxylate-bound **3**. The results of which revealed that, whereas 51% of **3** was bound to flüoride anions at **1** equiv of TBAF, 36% of **3** was found to form complexes with fluoride when 0.4 equiv of TBAF was added. These results suggest that TBAF could decrease the chain length of the supramolecular polymer when it was used as a competing anion. Initial support for that suggestion came from viscosity measurements. The relative viscosity of the 0.33 M **3** + TBAF solution was measured as 2.45, whereas the viscosity of **3** at the same concentration is 3.15 (Figure 3.4f). Additionally, a 0.51 M solution of **3** + TBAF was found not to show sol−gel transition at low temperatures (e.g., as low as -18 °C, Figure 3.5c), indicating the necessity of long supramolecular polymer chains to induce the sol−gel transition at low temperatures. Furthermore, DSC analysis of the aforementioned solution also did not show any transition between -20 and 10 °C,

supporting the above macroscopic observation. As a control experiment, the inverse vial test of a more concentrated cetyltrimethylammonium acetate solution (0.75 M in $CHCl_3$) did not show any sol−gel transition when the temperature of the solution decreased from 20 to 0 °C, contributing to the fact that supramolecular polymer formation is necessary to achieve rapid sol−gel transition.

3.3 Conclusion

In conclusion, we have prepared an AB-type linear supramolecular polymer capable of exhibiting rapid sol−gel transition induced by temperature. This supramolecular polymer contains cone-shaped π electron clouds formed via host−guest complexation between calix[4]pyrrole and its tethered carboxylate unit, key features that permit concurrent complexation of the countercation CTA. This, in turn, allows the supramolecular polymer as a whole to exhibit additional hydrophobic interactions and enables rapid sol−gel transition, which was supported by two-dimensional NMR and DSC measurement as well as SEM analysis. Considering the ease of synthesis of the monomer and high solubility of the subsequent supramolecular polymer, the present study illustrates the first example of rapid sol−gel transition behavior of an anion recognition based supramolecular polymer based on simultaneous ion pair recognition and van der Waals interactions. Our studies imply that ion pair recognition based supramolecular polymers can serve as a potential platform for the construction of fast responding smart materials.

3.4 Experimental Part

3.4.1 General information

Unless otherwise noted, all other commercially available reagents and solvents were used without further purification. The reaction progress was monitored on precoated silica gel TLC plates. Spots were visualized under 254 nm/365 nm UV light. ^{1}H, and ^{13}C, NOESY, ROESY and DOSY NMR spectra were recorded on an Agilent VNMRS 500 spectrometer using TMS as an internal reference. Mass spectra were measured on a Thermo Scientific TSQ Quantum GC and Micromass Autospec Ultima. A TA Q10 instrument was used to conduct DSC measurements in a flowing N_2 atmosphere at scanning rate of 20 ºC/min. Viscosity measurements were carried out with an

Ubbelohde micro dilution viscometer (Shanghai Liangjing Glass Instrument Factory, 0.40 mm inner diameter) at 293 K in chloroform. Compound **2** and CTAOH were synthesized according to previously reported literature procedures.

3.4.2 Synthesis

3.4.2.1 Compound 3

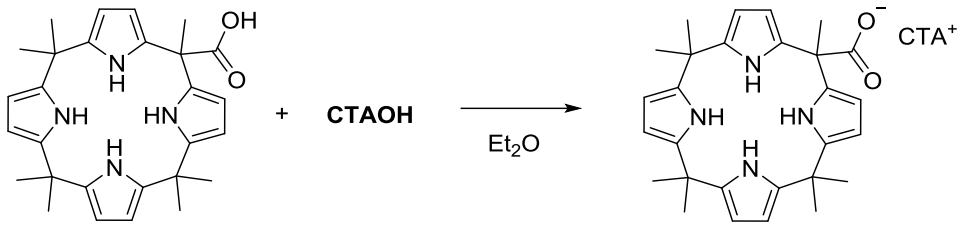

2 **3**

To a solution of **2** (617 mg, 1.35 mmol) dissolved in 150 mL diethyl ether, CTAOH (406 mg, 1.35 mmol) was added in one portion. The reaction mixture was stirred at room temperature for 1h. Addition of a few drops of acetonitrile caused the precipitation of the product which was filtered and washed with excess diethyl ether followed by drying under vacuum afforded **3** as a paleyellow solid (980 mg, 98%)

^{1}H NMR (500 MHz, $CDCl_3$, 25 °C): δ = 12.36 (2H, NH), 11.91 (2H, NH), 5.68 (2H, pyrrole-CH), 5.54 (m, 6H, pyrrole-CH), 2.21 (br t, 2H, –CH2–), 1.99 (s, 3H, –CH3), 1.90 (s, 3H, –CH3), 1.70 (br s, 2H, –CH2–), 1.66 (s, 3H, –CH3), 1.60 (6H, –CH3), 1.56 (6H, –CH3), 1.21-1.32 (br, m, 34H, $–CH_2$ and *meso*–CH_3), 0.89 (t, *J* = 6.8 Hz, 3H, $–CH_3$). ^{13}C NMR (126 MHz, $CDCl_3$): δ = 180.82, 141.69, 140.58, 139.25, 100.63, 99.62, 66.25, 50.86, 48.06, 34.77, 31.92, 29.69, 27.39, 27.01, 26.14, 22.69, 14.12. HRMS (ESI): m/z calcd for $C_{28}H_{33}N_4O_2$:457.26090; found: 457.26083 (as carboxylate salt in negative ionization mode).

4. HIGHLY SENSITIVE AND COST-EFFECTIVE FLUORESCENT TURN-ON IDA SENSORS BASED ON OCTOMETHYLCALIX[4]PYRROLE RECEPTOR FOR THE DETECTION OF FLUORIDE ANION[3]

4.1 Introduction

Fluoride exists at high levels in some ground waters, and used as an ingredient in some psychiatric drugs and anesthetics [61]. Insufficient and excess exposure of fluoride may cause inhibited tooth decay, bone disorder, and thyroid activity [62]. It also has active roles in the function of chemical warfare agents (e.g., Sarin, Tabun, and diisopropylfluorophosphate) and some insect poisons [63,64]. Therefore, selective sensing of fluoride ion was achieved by means of various optically active chemical platforms such as boron-dipyrromethane [65], urea [66], thiourea [67], hydrazone [68], dipyrromethene [69], and diketopyrrolopyrrole [70], to mention a few but a lot [71-77]. Most of these studies rely on coordination of target anion and report their presence via changes in the physical properties of the host such as color, fluorescence or phosphorescence. While most of these systems were designed based on indicator-spacer-receptor (ISR) approach, indicator-displacement assays (IDA) were also commonly used to overcome problems associated with ISR approach [78]. The displacement of indicator from a receptor by means of a competitive analyte was then evolved to fluorescent turn-on detection via the use of properly chosen fluorophores [78-81].

Among the various anion receptors, octamethylcalix[4]pyrrole (**1)** is particularly easy to preparethat can be synthesized in high yieldsthrough an acid catalyzed condensation reaction of pyrrole with acetone [82]. Its selectivity and sensory applications of its derivatives against F^- ion both in organic and aqueous media have been demonstrated in several occasions [83-91]. Although ISR approach was used in the design and

[3] This chapter is based on the paper ". Highly sensitive and cost-effective fluorescent turn-on sensors based on octamethylcalix[4]pyrrole receptor for the detection of fluoride" by Sana Amharar, Abdullah Aydoğan.2022, *Dyes and Pigments*,197,109918.

sensory applications of these systems, the recognition and colorimetric sensing of F^-ion in organic media was alsoaccomplished by Sessler and coworkerswith a colorimetric IDA composed of a **1**-(p-nitrophenolate) complex [92]. To overcome the low sensitivity of above system, Machado and co-workers used **1** and merocyanine dye as a colorimetric IDA assembly [33]. Additionally, Lee reported a symmetric "two-walled" calix[4]pyrrole IDA sensor displaying remarkable sensitivity and selectivity towards F^- ion [94]. Later on, Lee also reported anasymmetrically ''two-walled'' meso-substituted calix[4]pyrrole tethered by a fluorophore and its subsequent IDA implication as an archetype fluorescent turn-on single-molecular sensor which was shown to have a sub-nanomolar sensitivity against F^-ion [95].

Cost-effectiveness is another important parameter in the design and application of optical sensors. Although Lee and co-workers achieved selective sensing of F^-ion and gained good fidelities, their molecular systems require multistep reactions with moderate to considerable low yields in the preparation of cis-isomer of "two-walled" calix[4]pyrrole derivatives (e.g., 6%) which were used as the precursors of final IDA systems. Therefore, designing a simple and cost-effective calix[4]pyrrole IDA sensor that can be prepared in one easy synthetic step starting from commercially available materials and utilizing this IDA system in the selective optical sensing of F^- ion are among the aims of this work.

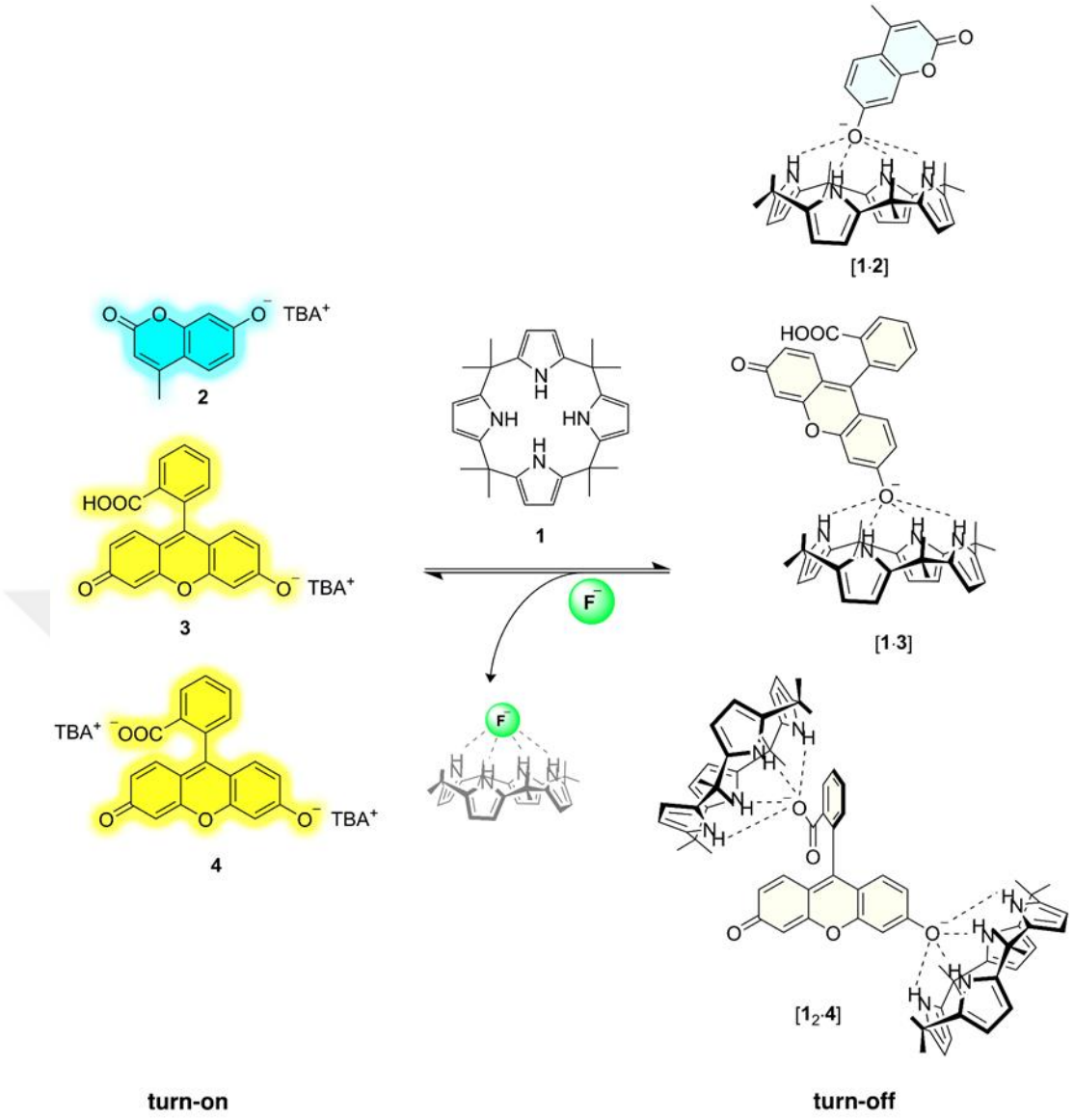

Figure 4.1 : Fluoride anion sensing pathways of IDA sensor composed of octamethylcalix[4]pyrrole (**1**) and TBA salts of 4-methylumbelliferone (**2**), and fluorescein (**3** and **4**).

4.2 Result and Discussion

4.2.1 Complexation studies

Initial complexation studies were carried out by means of ^{1}H NMR experiments. Chemical shift changes of pyrrole NH and CH protons belonging to **1** (15 mM) were tracked after addition of equimolar amount of **2** and **3**, separately in CD_3CN. As shown in Figure 4.2, a significant downfiled shift of pyrrole NH resonance signals was observed. Specifically, while the NH peaks resonate at 7.58 in the case of free **1**, they were found to shift 11.54 ppm after complexation with **2** (Figure 4.2b). In contrast to

what was observed for pyrrole NH resonance signals, pyrrole CH peaks showed an upfield shift from 5.83 ppm to 5.62 ppm.

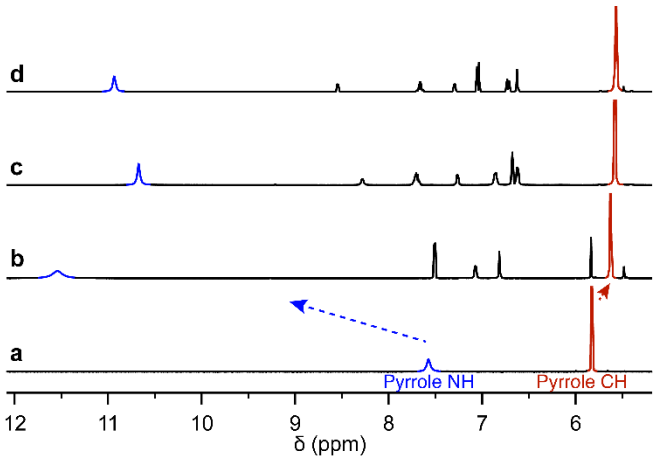

Figure 4.2 : Partial ^{1}H NMR spectra of (a) **1** (15 mM in CD_3CN), (b) equimolar mixtures of [**1**·**2**], (c) [**1**·**3**], and (d) [**1**$_2$·**4**].

These peak shifts are consistent with the formation of hydrogen bonds between pyrrole NHs of calix[4]pyrrole and phenolate anion.

Based on the results above, we have decided to test whether an IDA system could be prepared by using **1** and deprotonated forms of fluorescein (**3** and **4**). As anticipated, when equimolar **3** was added to a CD_3CN solution of **1** (15 mM), while the pyrrole NH peaks exhibited a downfield shift from 7.58 to 10.67 ppm, pyrrole CH protons revealed an upfield shift from 5.83 ppm to 5.58 ppm (Figure 4.2c). These results are similar to what was observed in the case of **2**, supporting the fact that **3** forms a complex through hydrogen bonding between its phenolate unit and calix[4]pyrrole NHs. Furthermore, pyrrole NH peaks of **1** were found to shift 10.93 ppm when bis-TBA salt of fluorescein (**4**) was complexed with two-fold excess of **1** (Figure 4.2d). Similar to above systems pyrrole CH resonance signals of [**1**$_2$·**4**] gave rise at an upper field corresponding to 5.57 ppm when compared with that of free **1**. These results were also allowed us to conclude that **1** is able to form a stable 1:2 complex after treatment with two-fold excess of **4**.

4.2.2 Binding constants

Binding constant determination studies between the receptor **1** and anionic dyes were also carried out in CD_3CN by using ^{1}H NMR titrations [100]. Results of which revealed that while the affinity constant between **1** and **2** was $7.21 \times 10^{4} \pm 1364\ M^{-1}$ it

was found to be $5.08 \times 10^4 \pm 50$ M^{-1} for [**1**·**3**]. In the case of [**1**$_2$·**4**], the first binding constant between carboxylate unit of **4** and **1** was calculated as $2.8 \times 10^5 \pm 31$ M^{-1} and the second affinity between phenolate part of **4** and **1** was found to be 1.9×10^3 $M^{-1} \pm$ 25.

4.2.3 Fluorescence turn-off experiments

Our simple sensor design consist of commercially available octamethylcalix[4]pyrrole (**1**) and easily deprotonated coumarin and fluorescein derivatives. As shown in Figure 4.3, while the compounds **2**, **3**, and **4** have strong fluorescence emission bands at 450, 531, and 534 nm, respectively, upon binding to calix[4]pyrrole cavity via hydrogen bonding, they exhibited notable fluorescence emission decreases because of possible photo-induced electron transfer from **1** to bound dyes [94].

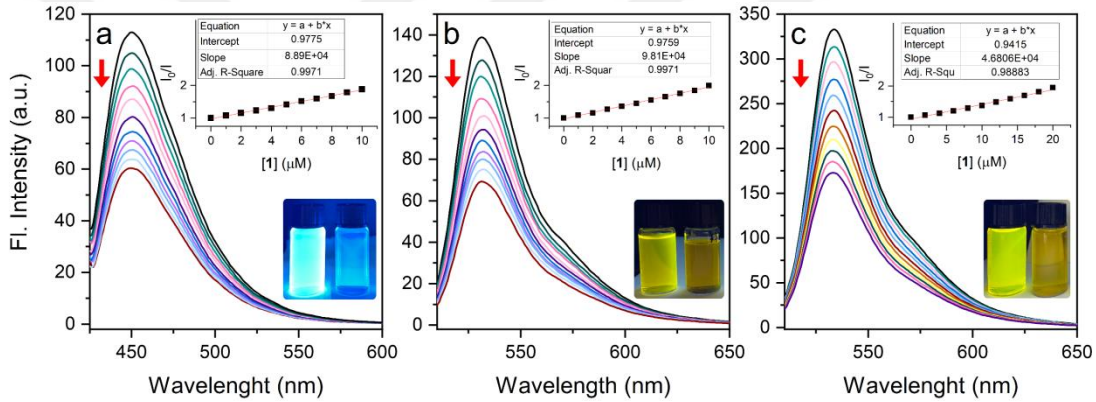

Figure 4.3 : Fluorescence quenching profiles of (a) **2** (10 μM) upon titration with **1** at λ_{max} = 450 nm, (b) **3** (10 μM) upon titration with **1** at λ_{max} = 531 nm, and (c) **4** (10 μM) upon titration with **1** at λ_{max} = 534 nm in CH_3CN.

The fluorescence diminutions were calculated to be 53, 50, and 52% for **2**, **3**, and **4**, respectively. The quenching efficiencies were thought to be effective as evident from the Stern-Volmer constants ($K_{SV} = 8.89 \times 10^4$ M^{-1} for **2**, 9.81×10^4 M^{-1} for **3**, and 4.68×10^4 M^{-1} for **4.**

4.2.4 Displacement analysis

In principle, original fluorescence of **2**–**4** will be recovered if calix[4]pyrrole bound dyes could be displaced by a target analyte anion. This requires a comparable binding affinity between analyte anion and receptor bound dyes. Specifically, the binding affinity between **1** and analyte needs to be sufficiently higher than that of **2**, **3**, and **4**. Hence, supramolecular displacement event could be utilized for the selective detection

of target analyte anion via fluorescence turn-on response.The displacement events were first monitored by ^{1}H NMR analyses. The binding constant between **1** and F^- was reported to be 1.62×10^6 in CH_3CN [41] which is stronger than that of **2**, **3**, and **4**. Therefore, we performed a series of ^{1}H NMR titrations to monitor the chemical shift changes of pyrrole NH peaks after treatment of equimolar amount of TBAF. Figure 4.4 clearly shows that addition of TBAF in to the CD_3CN solutions of complexes exhibited additional downfiled shifts in the pyrrole NH resonance signals.

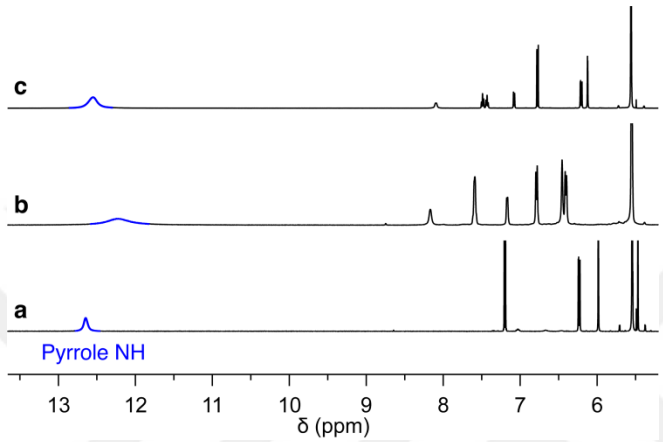

Figure 4.4 : Partial ^{1}H NMR spectra of (a) [**1**·**2**] + 1 equiv. TBAF, (b) [**1**·**3**] + 1 equiv. TBAF, and (c) [**1**$_2$·**4**] + 2 equiv. TBAF recorded in CD_3CN.

The Δδ values were calculated to be 1.11, 1.55, and 1.62 ppm for [**1**·**2**], [**1**·**3**], and [**1**$_2$·**4**] complexes, respectively, when related pyrrole NH resonance signals of Figure 4.2 and Figure 4.4 were compared. These results strongly suggest that [**1**·**2**], [**1**·**3**], and [**1**$_2$·**4**] complexes could be used as effective fluorescent turn-on sensors for F^- anion.

4.2.5 Sensing of F^-

To realize the expectations aforementioned above, calix[4]pyrrole complexes [**1**·**2**], [**1**·**3**], and [**1**$_2$·**4**] were titrated with F^- ion while keeping the concentrations of initial complexes constant. As shown in Figure 4.5, complete recovery of fluorescence responses was obtained upon incremental addition of F^- ion, confirming the stronger binding affinity of F^- with the receptor **1** compare to negatively charged dyes and the displacement of dyes from calix[4]pyrrole binding site during the formation of host-guest complex between **1** and F^-.

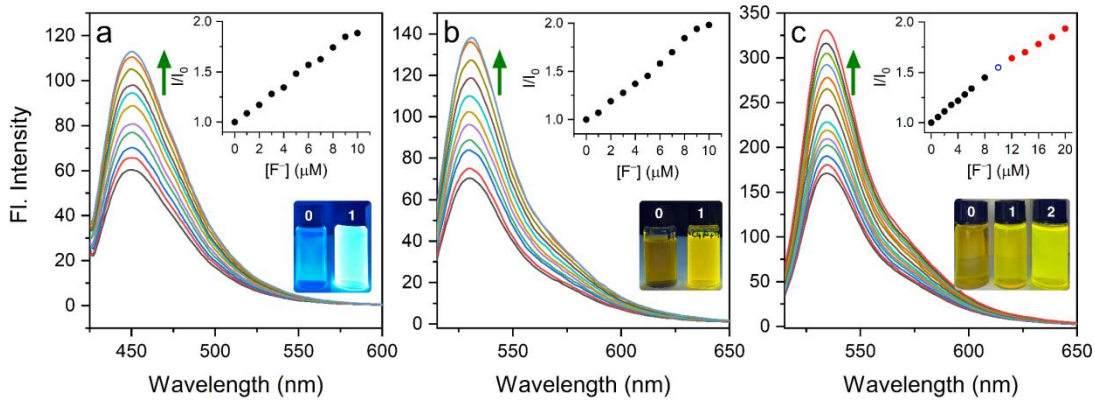

Figure 4.5 : Fluorescence responses of 10 μM solutions of (a) [**1**·**2**], (b) [**1**·**3**], and (c) [**1**$_2$·**4**] complexes upon titration with F^- ion (in the form of tetrabutylammonium salt) in CH_3CN at λ_{ex} = 420, 505 and 505 nm, respectively. Insets depict the plots of I/I_0 vs. F^- concentration and photographs of vials showing the fluorescence turn-on at 0, 1, and 2 equivalents of F^- concentrations.

For instance, while the emission intensity of [**1**·**2**] was initially 60.35, it was measured to be 113.84 after treatment with equimolar F^-, corresponding to the original emission intensity of **2** (Figure 4.5a). A recovery from 71.05 to 138.71 was also observed in the case of [**1**·**3**] complex when it was treated with F^- ion under the same conditions (Figure 4.5b). Similar trend was also obtained from [**1**$_2$·**4**] complex with an emission recovery from 170.34 to 330.79 (Figure 4.5c). Furthermore, the fluorescence enhancement profiles were found to be linear for all of the IDA systems. Hence, while the detection limit of [**1**·**2**] complex was found to be 67.1 nM, it was calculated to be 9.1 nM and 3.2 nM for [**1**·**3**] and [**12**·**4**] systems, respectively. Additional fluorescence titration experiments were also carried out in CH_3CN to study the interactions of **3** and **4** with F^- ion. A significant amount of emission enhancement was observed at 534 nm when 10 μM **3** was titrated with F^-. This was attributed to the deprotonation of carboxylic acid attached to **3** because of the basic character of fluoride [102,103]. In contrast, there was no significant change in the emission intensity at 534 nm when a 10 μM solution of **4** was titrated with F^- ion due to the lack of free proton in the carboxylic acid part of **4**. When the linearity in Figure. 4.5b up to 1 equiv. of F^-, extended F^- titration of [**1**·**3**] complex and the ^{1}H NMR titration results were taken into account it was concluded that while the displacement of **3** is effective up to one equivalent of F^-ion, deprotonation of free dye **3** is operative after further addition of F^-.

4.2.6 UV-vis studies

Unlike [**1**·**3**] and [**1**$_2$·**4**], UV-vis spectral perturbations were also observed when **2** was complexed with **1** and further displaced with F^- ion in CH_3CN. As shown in Figure 4.6, the absorption maximum of **2** was blue-shifted from 398 to 356 nm ($\Delta\lambda$ = 42 nm) after addition of equimolar **1**.

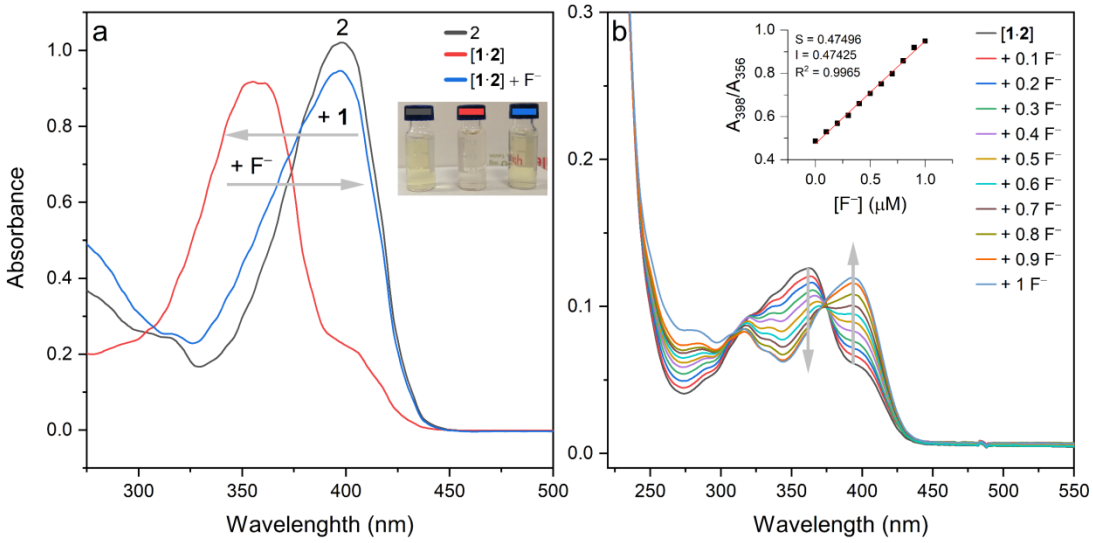

Figure 4.6 : UV-vis absorption maximum change of **2** (50 μM) upon complexation with **1** and after displacement with F^- ion. (b) Changes in the absorption spectrum of [**1**·**2**] (10 μM, CH_3CN) upon titration with TBAF.

Once the [**1**·**2**] complex was immediately formed, equimolar amount of TBAF was added into the complex solution to trigger the displacement event which was resulted a blue-shift back to the original absorption maximum of **2**. Systematic changes in absorption spectrum of [**1**·**2**] complex (10 μM) upon addition of F^- ion was also studied in CH_3CN as illustrated in Figure 4.6b. In consequent to incremental addition of F^-, absorption maximum was gradually red-shifted from 356 to 398 nm. An isosbestic point at 373 nm indicates the displacement of **2** from hydrogen binding site of **1**. Similar to what was obtained from its fluorescence turn on experiments, complex [**1**·**2**] exhibited a linear correlation between intensity ratios of absorption maxima at 398 nm to those at 356 nm (A_{398}/A_{356}) versus F^- ion concentration, demonstrating the potential utility of [**1**·**2**] complex in the determination of F^- concentration via UV-vis analysis. Absorption analysis was also utilized to test the selectivity of [**1**·**2**] complex towards F^- ion over a variety of other anions such as Cl^-, Br^-, I^-, $PhCO_2^-$, NO_3^-, SCN^-, CN^-, PF_6^-, $H_2PO_4^-$, and HSO_4^- (in the form of their tetrabutylammonium salts). Figure 4.7

shows the results of which and revealed that no significant absorbance perturbations or changes were observed during UV-vis experiments. Furthermore, while the addition of a mixture of analytes including Cl^-, Br^-, and I^- ions was not causing any remarkable changes in the absorbance of [**1**·**2**] complex, treatment of resultant mixture with F^- anion led to the same result what was observed in Figure 4.4b (Figure 4.7d).

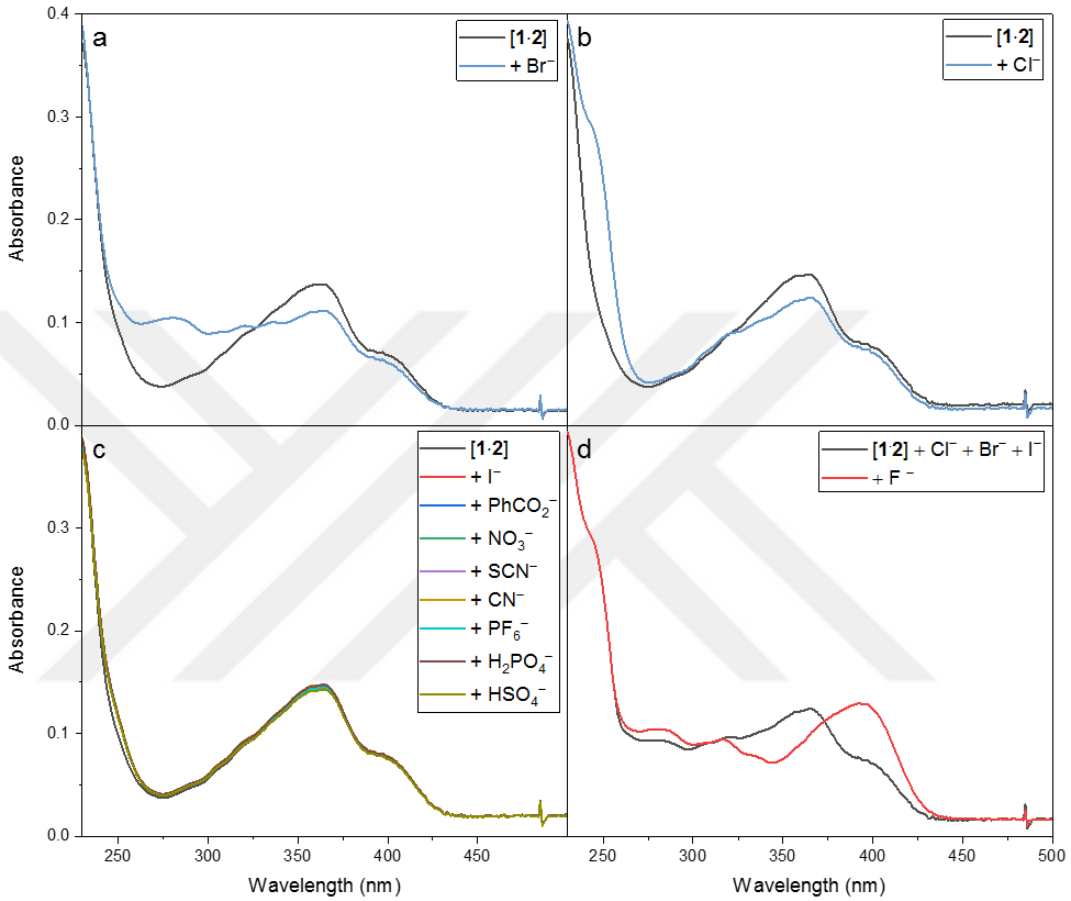

Figure 4.7 : UV-vis absorbance changes of [**1**·**2**] in CH_3CN after addition of equimolar amounts of anions (as their TBA salts): (a) Cl^-, (b) Br^-, (c) I^- and other anions. (d) UV-vis absorbance changes of [**1**·**2**] + Cl^-+ Br^-+ I^-in CH_3CN after treatment of equimolar F^- ion

These results strongly imply the necessity of such an anion that can form complex with receptor **1** way beyond stronger than **2** and the selectivity and specificity of [**1**·**2**] complex towards F^- ion over other anions studied.

4.2.7 Selectivity and competition

Fluorescence spectral measurements were also carried out to investigate the selectivity of [**1**·**2**], [**1**·**3**], and [$\mathbf{1}_2$·**4**] IDA sensors toward F^- ion. For that purpose, 10 μM CH_3CN solutions of sensors treated with equimolar amount of above aforementioned anions in

the form of their tetrabutylammonium salts. As illustrated in Figure. 4.8, while AcO^- and Cl^- anions were able to enhance the fluorescence emission intensities of IDA sensors a little, other anions (e.g., I^-, $PhCO_2^-$, NO_3^-, SCN^-, CN^-, PF_6^-, $H_2PO_4^-$, and HSO_4^-) did not cause any observable emission changes.eceptor **1** way beyond stronger than **2** and the selectivity and specificity of **[1·2]** complex towards F^- ion over other anions studied.

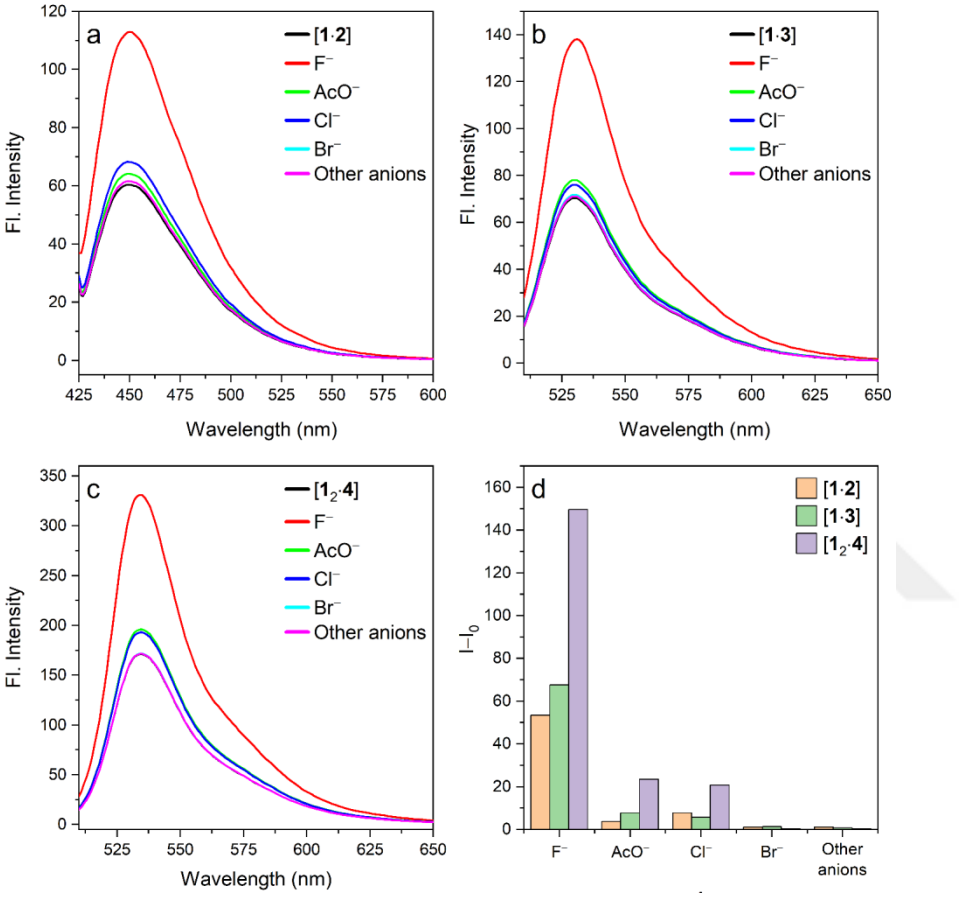

Figure 4.8 : Spectra and bar graphs (d) of fluorescence changes (where I_0 is initial intensities and I is final intensities) of (a) [**1**·**2**], (b) [**1**·**3**], and (c) [$\mathbf{1}_2$·**4**] complexes (10 μM in CH_3CN, λex = 420, 505, and 505 nm, respectively) upon addition of F^-, AcO^-,Cl^-, Br^- and other anions (10 μM).

In contrary, significant fluorescence enhancements were observed in the case of F^- ion. For instance, while [**1**·**2**] IDA sensor exhibited a 53.5 fluorescence enhancement, it was calculated to be 67.7 in the case of [**1**·**3**]. On the other hand, a 149.6 enhancement was observed in the case of [$\mathbf{1}_2$·**4**]. This apparent selectivity was attributed to the presence of two anionic domains in the structure of [$\mathbf{1}_2$·**4**] and requirement of two

equiv. F^- ion for complete displacement of calix[4]pyrrole units from the structure of IDA sensor.

The high selectivity toward F^- ion compare to other studied anions contributes a significant parameter to elucidate the performance of IDA sensors. Therefore, deviations in the fluorescence intensities were also studied when CH_3CN solutions of TBAF was mixed with the individual solutions of [**1**·**2**], [**1**·**3**], and [$\mathbf{1}_2$·**4**] in the presence of various anions. As illustrated in Figure. 4.9a-c, no significant enhancements were observed in emission spectra of IDA sensors except F^- ion.

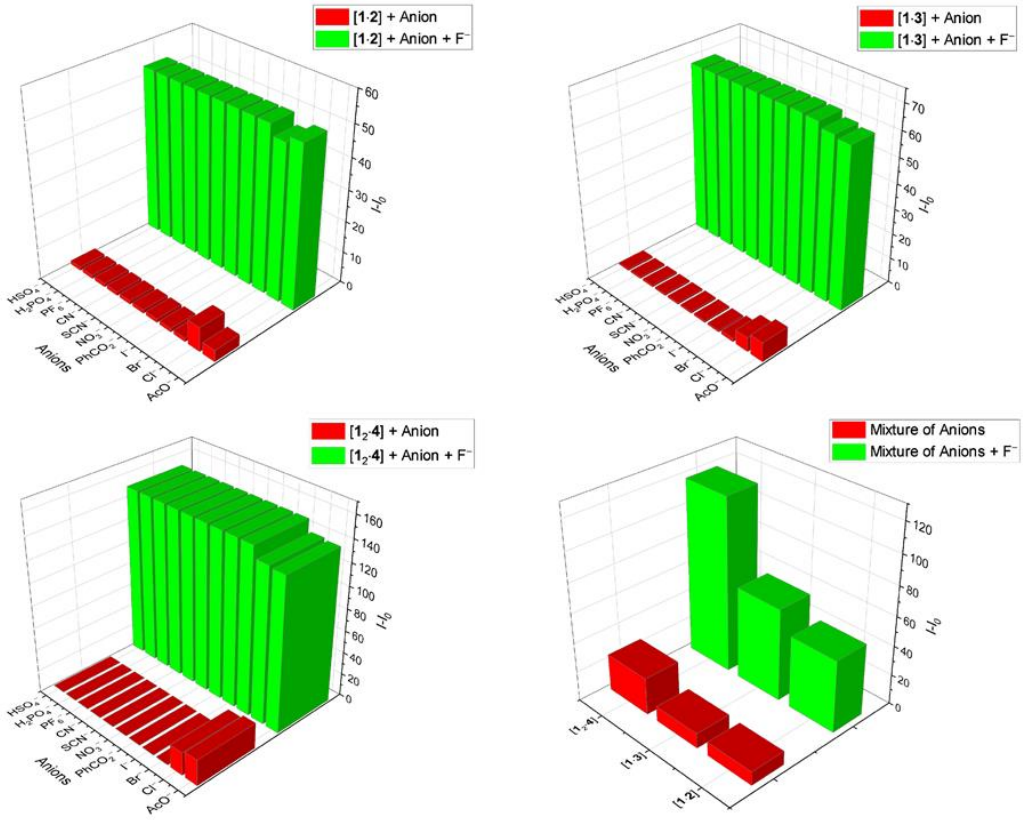

Figure 4.9 : Bar graphs of fluorescence responses in CH_3CN before and after addition of equimolar F^- ion: (a-c) IDA sensors (10 μM) + individual anions (10 μM), (d) IDA sensors (10 μM) + various anions (10 μM).

Additionally, in the presence of all the other anions studied in the same vessel, fluorescence emission enhancement changes were distinguishable after addition of F^- ion to the medium and the changes were almost similar to what was obtained from the single target fluorescence enhancements (Figure 4.9d).

4.2.8 Other solvent and reversibility

We also performed additional fluorescence measurement experiments in another solvent to test the extended application capability of IDA sensors. While **2**, **3**, and **4** were found to have slight solubilities in nonpolar solvents (e.g., methylene chloride and diethyl ether) they exhibited good solubilities in polar solvents such as tetrahydrofuran (THF), dimethyl sulfoxide, and acetone. Therefore, THF was chosen as an alternate solvent to carry out fluorescence perturbation experiments. As shown in Figure 4.10, when THF solutions of **2** (10 μM, λ_{ex} = 345 nm), **3** (30 μMλ_{ex} = 545 nm), and **4** (30 μM, λ_{ex} = 545 nm) were individually treated with equimolar amount of **1**, distinguishable fluorescence emission diminishes were observed due to the formation host-guest complexes between the indicators and the receptor **1**.

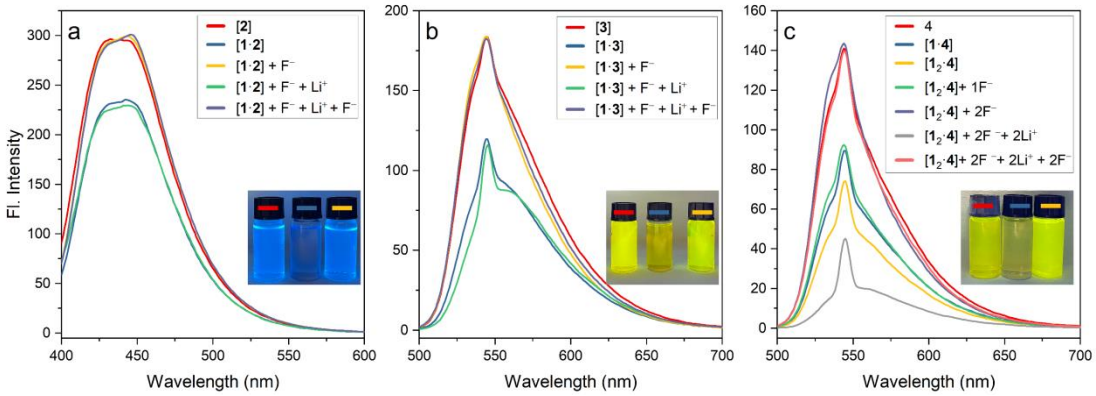

Figure 4.10 : Fluorescence emission spectra of **2** (a), **3** (b), and **4** (c) before and after sequential addition of equimolar **1**, F^-, Li^+, and again F^- in THF. Insets shows the photographs of indicators (red bars) and their turn-off and turn-on behaviors after treatment with **1** (blue bars) and F^- anion (yellow bars), respectively.

Further addition of F^- anion to the resultant mixtures resulted turn-on events in the fluorescence emissions. These findings clearly show that the IDA sensors [**1**·**2**], [**1**·**3**], and [$\mathbf{1}_2$·**4**] exhibit behaviors similar to CH_3CN solutions and they could be utilized for the detection of F^- anion in THF as well.

The reversibility of binding F^- to the IDA sensors was also examined in THF solutions containing equimolar Li^+ (as ClO_4^- salt) was added to fluoride treated solutions (Figure 4.10 yellow bars) of [**1**·**2**], [**1**·**3**], and [$\mathbf{1}_2$·**4**]. Figure 4.10 also shows the results of which and reveals that the added Li^+ ions reacts with the calix[4]pyrrole bound F^- anions and the resulting free calix[4]pyrroles reassembles the IDA sensors back again. These

phenomena were reflected in the fluorescence spectra as turn-off events (Figure. 4.10 green bars) for [**1**·**2**], [**1**·**3**], and [$\mathbf{1}_2$·**4**]. Further treatment of reassembled IDA sensors with equimolar amount of F^- ion triggers the fluorescence turn-on events (Figure. 4.10 gray bars) back to the initial intensity values. This reversibility cycles have been successfully repeated up to three times. The above results allowed us to conclude that the IDA sensors [**1**·**2**], [**1**·**3**], and [$\mathbf{1}_2$·**4**] can be used reversibly to detect F^- anion.

4.3 Experimental Part

4.3.1 Chemical and apparatus

Unless specifically indicated, all chemicals and solvents used in this study were purchased from commercial sources and used as received. Compounds **1** was prepared according to literature procedure [98]. ^{1}H and ^{13}C NMR spectra were used in the characterization of products recorded on an Agilent VNMRS 500 MHz nuclear magnetic resonance spectrometer using a residual protio solvent as the reference. UV–vis spectra were recorded on a Shimadzu 3100 spectrometer. Fluorescence measurements were carried out with an Agilent Cary Eclipse fluorescence spectrophotometer using a conventional cell with 1 cm path length. Mass spectra were measured on a Thermo Scientific TSQ Quantum GC and Micromass Autospec Ultima.

4.3.2 Synthesis of TBA salts

TBA salt of **2** was prepared according to literature procedure [99]. TBA salts of fluorescein were prepared as detailed below: To methanol solutions of fluorescein (0.6 mmol) was added equimolar amount (two equivalents were used in the case of **4**) of tetrabutylammonium hydroxide (1M, in MeOH). The reaction mixture was then stirred for 2 hours at room temperature. After evaporation of methanol, the products were triturated in diethyl ether and dried under vacuum at 40 °C to afford desired TBA^+ salts **3** and **4**.

3: ^{1}H NMR (500 MHz, CD_3CN,): δ = 8.11 (dd, *J* = 7.4, 1.7 Hz, 1H), 7.61 – 7.54 (m, 2H), 7.20 – 7.16 (m, 1H), 6.82 (d, *J* = 9.1 Hz, 2H), 6.50 – 6.37 (m, 2H), 6.32 (dd, *J* = 9.2, 2.2 Hz, 2H), 3.13 – 3.03 (m, 8H), 2.72 (br, 1H), 1.60 (p, *J* = 7.8 Hz, 8H), 1.35 (h, *J* = 7.5 Hz, 8H), 0.97 (t, *J* = 7.3 Hz, 12H); ^{13}C NMR (126 MHz, $CDCl_3$) δ = 207.1,

170.3, 156.7, 130.6, 128.8, 128.2, 103.2, 58.6, 53.4, 50.6, 30.9, 23.8, 19.6, 15.3, 13.6; HRMS (ESI): m/z calcd for $C_{20}H_{11}O_5$ $[M]^-$: 331.06120; found: 331.06125.

4: ^{1}H NMR (500 MHz, CD_3CN) δ = 8.04 – 7.99 (m, 1H), 7.44 (td, *J* = 7.5, 1.4 Hz, 1H), 7.37 (td, *J* = 7.4, 1.5 Hz, 1H), 7.07 – 7.01 (m, 1H), 6.72 (d, *J* = 9.3 Hz, 2H), 6.13 (dd, *J* = 9.3, 2.1 Hz, 2H), 6.03 (d, *J* = 2.2 Hz, 2H), 3.18 – 3.06 (m, 16H), 1.67 – 1.55 (m, 16H), 1.36 (q, *J* = 7.4 Hz, 16H), 0.98 (t, *J* = 7.4 Hz, 24H); ^{13}C NMR (126 MHz, $CDCl_3$) δ 181.5, 170.6, 158.5, 158.3, 142.4, 133.6, 131.3, 130.3, 129.1, 128.1, 127.3, 123.2, 110.5, 103.5, 58.6, 23.9, 19.6, 13.7; HRMS (ESI): m/z calcd for $C_{52}H_{83}N_2O_5$ $[M-H]^-$: 815.62965; found: 815.62971.

4.3.3 Complexation experiments and binding constant determination

NMR spectroscopy was utilized to conduct the complexation and binding constant determination experiments at 25 °C in deuterated acetonitrile. 15 mM **1** and equimolar amount of dyes (**2**, **3**, and **4**) were used while monitoring the chemical shift changes of pyrrole–NH and –CH– proton signals. Binding constant measurements were also carried out in deuterated acetonitrile at a constant temperature of 25 °C. During these experiments the concentration of host **1** was kept constant while increasing the equivalents of guest species **2**, **3**, and **4**. Changes in the chemical shifts of pyrrole–NH protons belonging to **1** were used to calculate the binding constants with the aid of Bindfit [100].

4.3.4 Preparation of solutions for spectral measurements

All UV-vis and fluorescence titration experiments were performed at room temperature. To carry out spectral measurements, 1.0×10^{-3} M stock solutions of **1**, **2**, **3**, **4** and anions (in the form of their tetrabutylammonium salts) were prepared in CH_3CN. Required dilutions were then performed based on the conditions of the desired spectral measurement. For the fluorescence turn-off and UV-vis experiments, 10 μM of receptor **1** was titrated with individual CH_3CN solutions of **2**, **3**, and **4** while keeping the concentration of **1** constant. During fluorescence turn-on and selectivity experiments 10 μM CH_3CN solutions of **[1·2]**, **[1·3]**, and **[1_2·4]** (in the case of THF the concentrations of **[1·3]**, and **[1_2·4]** was 30 μM) titrated with desired anion solution while keeping the concentrations of IDA systems constant.

4.3.5 Detection limit determination

The following equation was used to calculate the detection limit based on the fluorescence titration:

$$Detection\ limit = 3\sigma/k$$

where σ is the standard deviation of blank signals and *k* is the slope of linear calibration plots. Fluorescence emission spectra of **2**, **3**, and **4** were measured ten times and σ values were calculated. The slope values were obtained after plotting emission changes of **[1·2]**, **[1·3]**, and **[1_2·4]** upon F^- ion addition at λ_{max} wavelengths as a function of concentration. 5 nm emission slit width was employed during detection limit calculation experiments.

4.4 Conclusion

The present findings illustrate that a commercially available host scaffold octamethylcalix[4]pyrrole receptor (**1**) and 4-methylumbelliferone (**2**) or fluorescein indicators (**3** and **4**, in the form of their TBA salts) could be used to produce highly sensitive and reversible fluorescence turn-on IDA sensors that can report the presence of fluoride anion in acetonitrile and THF. The current system also provides a simple and cost-effective IDA platform to discriminate fluoride anion when the sensors were exposed to a mixture of studied anions. It was also found that the IDA sensor composed of octamethylcalix[4]pyrrole and bis-TBA salt of fluorescein (**1_2·4**) could be used for the sensing of fluoride anion with a very low detection limit.

5. CONCLUSION

In conclusion, in chapter two we have illustrated the first example of a high performance supramolecular polymer and its gelation based on the anion recognition chemistry of calix[4]pyrrole. In chapter three, we demonstrated the first example of rapid sol-gel transition behavior of supramolecular polymer based on both ion pair recognition and van der Waals interactions which can find utility in the futurefor the development of platforms for smart materials.

And finally, we have illustrated that a commercially available host scaffold octamethylcalix[4]pyrrole receptor and TBA salts of 4-methylumbelliferone or fluorescein indicators could be used to produce highly sensitive and reversible fluorescence turn-on IDA sensors that can report the presence of very low concentration of fluoride anion in various organic solvents.

REFERENCES

[1] **Yang, L., Tan, X., Wang, Z., & Zhang, X.** (2015). Supramolecular Polymers: Historical Development, Preparation, Characterization, and Functions. *Chemical Reviews*, *115*(15), 7196-7239.

[2] **Yan, X., Wang, F., Zheng, B., & Huang, F.** (2012). Stimuli-responsive supramolecular polymeric materials. *Chemical Society Reviews, 41*(18), 6042-6065.

[3] **Gibson, H. W., Yamaguchi, N., Niu, Z., Jones, J. W., Slebodnick, C., Rheingold, A. L., & Zakharov, L. N.** (2010). Self-assembly of daisy chain oligomers from heteroditopic molecules containing secondary ammonium ion and crown ether moieties. *Journal of Polymer Science Part A: Polymer Chemistry, 48*(4), 975-985.

[4] **Guo, D. S., & Liu, Y**. (2012). Calixarene-based supramolecular polymerization in solution. *Chemical Society Reviews, 41***(**18), 5907-5921.

[5] **Harada, A., Takashima, Y., & Yamaguchi, H.** (2009). Cyclodextrin-based supramolecular polymers. *Chemical Society Reviews, 38*(4), 875-882.

[6] **Qian, H., Guo, D. S., & Liu, Y**. (2012). Cucurbituril-Modulated Supramolecular Assemblies: From Cyclic Oligomers to Linear Polymers. *Chemistry-a European Journal, 18*(16), 5087-5095.

[7] (a) **Li, C**. (2014). Pillararene-based supramolecular polymers: from molecular recognition to polymeric aggregates. *Chemical Communications, 50*(83), 12420-12433.

[8] **Gale, P. A., Sessler, J. L., Kral, V., & Lynch, V**. (1996). Calix[4]pyrroles: Old yetnew anion-binding agents. *Journal of the American Chemical Society*, *118*(21), 5140-5141.

[9] (a) **Sun, Q., Lü, Y., Liu, L., Liu, K., Miao, R., & Fang, Y.** (2016). Experimental Studies on A New Fluorescent Ensemble of Calix[4]pyrrole and Its Sensing Performance in the Film State. *ACS Applied Materials & Interfaces, 8*(42), 29128-29135

[10] **Aydogan, A., Koca, A., Şener, M. K., & Sessler, J. L.** (2014). EDOT-Functionalized Calix[4]pyrrole for the Electrochemical Sensing of Fluoride in Water. *Organic Letters, 16*(14), 3764.

[11] **Aydogan, A.** (2016). Synthesis and characterisation of a calix[4]pyrrole functional polystyrene via 'click chemistry' and its use in the extraction of halide anion salts. *Supramolecular Chemistry, 28*(1-2), 117-124. (b).

[12] **Clarke, H. J., Howe, E. N. W., Wu, X., Sommer, F., Yano, M., Light, M. E… Gale, P. A**. (2016). Transmembrane Fluoride Transport: Direct Measurement and Selectivity Studies. *Journal of the American Chemical Society, 138* (50), 16515-16522.

[13] **Kim, D. S., & Sessler, J. L.** (2015). Calix[4]pyrroles: versatile molecular containers with ion transport, recognition, and molecular switching functions. *Chemical Society Reviews, 44*(2), 532-546.

[14] **Aydogan, A., Lee, G., Lee, C.-H., & Sessler, J. L.** (2015). Reversible Assembly and Disassembly of Receptor-Decorated Gold Nanoparticles Controlled by Ion Recognition. *Chemistry – A European Journal, 21*(6), 2368-2376.

[15**] Park, J. S., Yoon, K. Y., Kim, D. S., Lynch, V. M., Bielawski, C. W., Johnston, K. P., & Sessler, J. L.** (2011). Chemoresponsive alternating supramolecular copolymers created from heterocomplementary calix[4]pyrroles. *Proceedings of the National Academy of Sciences, 108*(52), 20913-20917.

[16] **Bähring, S., Martín-Gomis, L., Olsen, G., Nielsen, K. A., Kim, D. S., Duedal, T… Sessler, J. L.** (2016). Design and Sensing Properties of a Self-Assembled Supramolecular Oligomer. *Chemistry – A European Journal, 22*(6), 1958-1967.

[17] **Aydogan, A., & Sessler, J. L.** (2014). An imidazolium-functionalized self-assembling calix[4]pyrrole. *Chemical Communications, 50*(88), 13600-13603

[18] **Sessler, J. L., Cho, W. S., Gross, D. E., Shriver, J. A., Lynch, V. M., & Marquez, M.** (2005). Anion binding studies of fluorinated expanded calixpyrroles. *Journal of Organic Chemistry, 70*(15), 5982-5986.

[19] **Yamaguchi, N., Nagvekar, D. S., & Gibson, H. W.** (1998). Self-Organization of a Heteroditopic Molecule to Linear Polymolecular Arrays in Solution. *Angewandte Chemie International Edition, 37*(17), 2361-2364.

[20**] Aydogan, A., Sessler, J. L., Akar, A., & Lynch, V.** (2008). Calix[4]pyrroles with long alkyl chains: Synthesis, characterization, and anion binding studies. *Supramolecular Chemistry, 20*(1-2), 11-21.

[21] CCDC 1583877 (3b.2(CH3CN)) contains the supplementary crystallographic data for this paper. This data is provided free of charge by The Cambridge Crystallographic Data Center.

[22] **Gale, P. A., Sessler, J. L., & Král, V.** (1998). Calixpyrroles. *Chemical Communications*(1), 1-8. (b) **Gale, P. A., Anzenbacher Jr, P., & Sessler, J. L**. (2001). Calixpyrroles II. *Coordination Chemistry Reviews, 222*(1), 57-102.

[23] **Saha, I., Lee, J. H., Hwang, H., Kim, T. S., & Lee, C.-H.** (2015). Remarkably selective, non-linear allosteric regulation of anion binding by a tetracationic calix[4]pyrrole homodimer. *Chemical Communications, 51*(26), 5679-5682.

[24] **Xu, J.-F., Huang, Z., Chen, L., Qin, B., Song, Q., Wang, Z., & Zhang, X.** (2015). Supramolecular Polymerization Controlled by Reversible Conformational Modulation. *ACS Macro Letters, 4*(12), 1410-1414.

[25] **Liu, Y., Wang, Z., & Zhang, X**. (2012). Characterization of supramolecular polymers. *Chemical Society Reviews, 41*(18), 5922-5932.

[26] **Li, Z.-Y., Zhang, Y., Zhang, C.-W., Chen, L.-J., Wang, C., Tan, H… Yang, H.-B**. (2014). Cross-Linked Supramolecular Polymer Gels Constructed from Discrete Multi-pillar[5]arene Metallacycles and Their Multiple Stimuli-Responsive Behavior. *Journal of the American Chemical Society*, *136*(24), 8577-8589.

[27] **Wang, F., Zhang, J., Ding, X., Dong, S., Liu, M., Zheng, B… Huang, F**. (2010). Metal Coordination Mediated Reversible Conversion between Linear and Cross-Linked Supramolecular Polymers. *Angewandte Chemie International Edition*, *49*(6), 1090-1094.

[28] **Sessler, J. L., Andrievsky, A., Gale, P. A., & Lynch, V.** (1996). Anion Binding: Self-Assembly of Polypyrrolic Macrocycles. *Angewandte Chemie International Edition*, *35*(23-24), 2782-2785.

[29] **Martin, R. B.** (1996). Comparisons of Indefinite Self-Association Models. *Chemical Reviews*, *96*(8), 3043-3064.

[30] **Gotor, R.; Costero, A. M.; Gil, S.; Gaviña, P.; Rurack, K.** (2014) On the Ion-Pair Recognition and Indication Features of a Fluorescent Heteroditopic Host Based on a BODIPY Core. *Eur. J. Org. Chem.*, *2014* (19), 4005-4013.

[31] **Webber, P. R. A.; Beer, P. D**. (2003) Ion-pair recognition by a ditopic calix[4]semitube receptor. *Dalton Trans.*, (11), 2249-2252.

[32] **Chi, X.; Peters, G. M.; Hammel, F.; Brockman, C.; Sessler**, **J. L** (2017). Molecular Recognition Under Interfacial Conditions: CaliX[4]pyrrole-Based Cross-linkable Micelles for Ion Pair EXtraction. *J. Am. Chem. Soc.*, *139* (27), 9124−9127.

[33**] Adriaenssens, L.; Estarellas, C.; Vargas Jentzsch, A.; Martinez Belmonte, M.; Matile, S.; Ballester**, **P** (2013). Quantification of Nitrate−π Interactions and Selective Transport of Nitrate Using Calix[4]pyrroles with Two Aromatic Walls. *J. Am. Chem. Soc.*, *135* (22), 8324-8330.

[34] **Kim, S. K.; Sessler, J. L.; Gross, D. E.; Lee, C.-H.; Kim, J. S.; Lynch, V. M.; Delmau, L. H.; Hay, B. P.** (2010) A Calix[4]arene Strapped Calix[4]pyrrole: An Ion-Pair Receptor Displaying Three Different Cesium Cation Recognition Modes. *J. Am. Chem. Soc.*, *132* (16), 5827-5836

[35] **Barea, E.; Navarro, J. A. R.; Salas, J. M.; Masciocchi, N.; Galli, S.; Sironi, A.** (2004). Mineralomimetic Sodalite- and Muscovite-Type Coordination Frameworks. Dynamic Crystal-to-Crystal Interconversion Processes Sensitive to Ion Pair Recognition. *J. Am. Chem. Soc.*,*126* (10), 3014-3015.

[36] **He, Q.; Vargas-Zúñiga, G. I.; Kim, S. H.; Kim, S. K.; Sessler, J. L.** (2019). Macrocycles as Ion Pair Receptors. *Chem. Rev.*, *119* (17), 9753-9835.

[37] **McConnell, A. J.; Docker, A.; Beer, P. D.** (2020). From Heteroditopic to Multitopic Receptors for Ion-Pair Recognition: Advances in Receptor Design and Applications. *ChemPlusChem*, *85* (8), 1824-1841.

[38] **Custelcean, R.; Delmau, L. H.; Moyer, B. A.; Sessler, J. L.; Cho, W. S.; Gross, D…Gale, P. A.** (2005). Calix[4]pyrrole: An old yet new ion-pair receptor. *Angew. Chem., Int. Ed.***,** *44* (17), 2537-2542.

[39] **Caltagirone, C.; Bill, N.; Gross, D.; Light, M.; Sessler, J.; Gale, P.** (2010). Bis-cation salt complexation by meso-octamethylcalix[4]pyrrole: linking complexes in solution and in the solid state. *Org. Biomol. Chem.*, *8* (1), 96-99.

[40] **Molina-Muriel, R.; Aragay, G.; Escudero-Adan, E. C.; Ballester, P.** (2018). Switching from Negative-Cooperativity to No-Cooperativity in the Binding of Ion-Pair Dimers by a Bis(calix[4]pyrrole) Macrocycle. *J Org Chem***,** *83* (21), 13507-13514.

[41] **Lee, C. H.; Miyaji, H.; Yoon, D. W.; Sessler, J. L.** (2008). Strapped and other topographically nonplanar calixpyrrole analogues. Improved anion receptors. *Chem. Commun.*, (1), 24-34.

[42] **Romero, J. R.; Aragay, G.; Ballester, P.** (2017). Ion-pair recognition by a neutral [2]rotaxane based on a bis-calix[4]pyrrole cyclic component. *Chem. Sci.*, *8* (1), 491-498.

[43**] Kim, S. K.; Sessler, J. L**. (2010) Ion pair receptors. *Chem. Soc. Rev***.,** *39* (10), 3784-3809.

[44] **Ciardi, M.; Galán, A.; Ballester, P.** (2015). Tetra-phosphonate Calix[4]pyrrole Cavitands as Multitopic Receptors for the Recognition of Ion Pairs. *J. Am. Chem. Soc.*, *137* (5), 2047-2055.

[45] **Hollamby, M. J.; Karny, M.; Bomans, P. H. H.; Sommerdjik, N. A. J. M.; Saeki, A.; Seki, S… Nakanishi, T.** (2014). Directed assembly of optoelectronically active alkyl–π-conjugated molecules by adding n-alkanes or π-conjugated species. *Nature Chemistry***,** *6* (8), 690-696.

[46] **Sessler, J. L.; Cho, W. S.; Gross, D. E.; Shriver, J. A.; Lynch, V. M.; Marquez, M**. (2005) Anion binding studies of fluorinated expanded calixpyrroles. *J. Org. Chem. 70* (15), 5982-5986.

[47] **Yamaguchi, N.; Nagvekar, D. S.; Gibson, H. W**. (1998) Self-Organization of a Heteroditopic Molecule to Linear Polymolecular Arrays in Solution. *Angew. Chem., Int. Ed., 37* (17), 2361-2364.

[48**] Amharar, S.; Yuvayapan, S.; Aydogan, A**. (2018). A thermoresponsive supramolecular polymer gel from a heteroditopic calix[4]pyrrole. *Chem. Commun.***,** *54* (7), 829-832.

[49] **Aydogan, A.; Sessler, J. L.; Akar, A.; Lynch, V.** (2008). Calix[4]pyrroles with long alkyl chains: Synthesis, characterization, and anion binding studies. *Supramol. Chem., 20* (1−2), 11−21.

[50] **Gale, P. A.; Sessler, J. L.; Kral, V.; Lynch, V.** (1996). Calix[4]pyrroles:Old yet new anion-binding agents. *J. Am. Chem. Soc., 118* (21), 5140−5141.

[51] **Sessler, J. L.; Andrievsky, A.; Gale, P. A.; Lynch, V**. (1996). AnionBinding: Self-Assembly of Polypyrrolic Macrocycles. *Angew. Chem., Int. Ed. Engl*., *35* (23−24), 2782−2785.

[52] **Xu, J.-F.; Huang, Z.; Chen, L.; Qin, B.; Song, Q.; Wang, Z.;Zhang, X.** (2015). Supramolecular Polymerization Controlled by Reversible Conformational Modulation. *ACS Macro Lett*., *4* (12), 1410−1414.

[53] **Yang, X.; Cai, W.; Dong, S.; Zhang, K.; Zhang, J.; Huang, F.; Huang, F.; Cao, Y.** (2017). Fluorescent Supramolecular Polymers Based on Pillar[5]arene for OLED Device Fabrication. *ACS Macro Lett.*, *6* (7), 647−651.

[55] **Wei, P.; Yan, X.; Cook, T. R.; Ji, X.; Stang, P. J.; Huang, F.** (2016). Supramolecular Copolymer Constructed by Hierarchical Self-Assembly of Orthogonal Host−Guest, H-Bonding, and Coordination Interactions. *ACS Macro Lett.*, *5* (6), 671−675.

[56] **Shi, X.; Zhang, X.; Ni, X.-L.; Zhang, H.; Wei, P.; Liu, J.; … Tang,B. Z. (**2019). Supramolecular Polymerization with Dynamic Self-Sorting Sequence *Control. Macromolecules*, *52* (22), 8814−8825.

[57] **Liu, Y.; Wang, Z.; Zhang, X.** (2012). Characterization of supramolecular polymers.*Chem. Soc. Rev.*, *41* (18), 5922−5932.

[58] **Yuvayapan, S.; Aydogan, A.** (2019). Counter Cation Dependent andStimuli Responsive Supramolecular Polymers Constructed by Calix[4]pyrrole Based Host-Guest Interactions. *Eur. J. Org. Chem. 2019*, (4), 633−639.

[59] **Gale, P. A.; Sessler, J. L.; Kraĺ, V.** (1998). Calixpyrroles. *Chem. Commun*., *1*, 1−8.

[60] **Gale, P. A.; Anzenbacher, P., Jr; Sessler, J. L**. (2001). Calixpyrroles II.Coord. *Chem. Rev*., *222* (1), 57−102.

[61] **E.M. Sakai, L.A. Connolly, J.A. Klauck**. (2005). Inhalation Anesthesiology and Volatile Liquid Anesthetics: Focus on Isoflurane, Desflurane, and Sevoflurane, Pharmacotherapy: *The Journal of Human Pharmacology and Drug Therapy*,*25* 1773-1788.

[62] **S. Ayoob, A.K. Gupta**. (2006). Fluoride in drinking water: A review on the status and stress effects, *Crit. Rev. Env. Sci. Technol*., *36* 433-487.

[63] **C.B. Millard, G. Kryger, A. Ordentlich, H.M. Greenblatt, M. Harel, M.L. Raves…J.L. Sussman.** (1999). Crystal Structures of Aged Phosphonylated Acetylcholinesterase: Nerve Agent Reaction Products at the Atomic Level, *Biochemistry*, *38* 7032-7039

[64] **S.-W. Zhang, T.M. Swager**. (2003) Fluorescent Detection of Chemical Warfare Agents: Functional Group Specific Ratiometric Chemosensors, *J. Am. Chem. Soc*., *125* 3420-3421.

[65] **X. Chen, Y.-C. Liu, J. Bai, H. Fang, F.-Y. Wu, Q. Xiao**. (2021) A "turn-on" fluorescent probe based on BODIPY dyes for highly selective detection of fluoride ions, *DyesPigm.*190109347.

[66] **V. Amendola, G. Bergamaschi, M. Boiocchi, L. Fabbrizzi, L. Mosca**, (2013) The Interaction of Fluoride with Fluorogenic Ureas: An ON1–OFF–ON2 Response, *J. Am. Chem. Soc*., *135* 6345-6355,

[67] **B. Zavala-Contreras, H. Santacruz-Ortega, A.U. Orozco-Valencia, M. Inoue, K. Ochoa Lara, R.-E. Navarro.** (2021). Optical Anion Receptors with

Urea/Thiourea Subunits on a TentaGel Support, *ACS Omega, 6* 9381-9390.

[68] **S. Mukherjee, A.K. Paul, H. Stoeckli-Evans.** (2014). A family of highly selective fluorescent sensors for fluoride based on excited state proton transfer mechanism, *Sens. Actuators B: Chem., 202* 1190-1199.

[69] **J.-M. You, H. Jeong, H. Seo, S. Jeon.** (2010). A new fluoride ion colorimetric sensor based on dipyrrolemethanes, Sens. Actuators B: Chem., *146* 160-164.

[70] **X. Yang, L. Xie, R. Ning, X. Gong, Z. Liu, Y. Li, L. Zheng, …G. Zhang.** (2015) A diketopyrrolopyrrole-based near-infrared sensor for selective recognition of fluoride ions, *Sens. Actuators B: Chem., 210* 784-794.

[71] **A. Aydogan, G. Lee, C.-H. Lee, J.L. Sessler**. (2015). Reversible Assembly and Disassembly of Receptor-Decorated Gold Nanoparticles Controlled by Ion Recognition, *Chem. Eur. J., 21* 2368-2376.

[72] **E. Baysak, S. Yuvayapan, A. Aydogan, G. Hizal**, (2018) Calix[4]pyrrole-decorated carbon nanotubes on paper for sensing acetone vapor, *Sens. Actuators B Chem, 258* 484-491.

[73] **Y. Zhou, J.F. Zhang, J. Yoon.** (2014). Fluorescence and Colorimetric Chemosensors for Fluoride-Ion Detection, *Chem. Rev., 114* 5511-5571.

[74] **S. Dhiman, M. Ahmad, N. Singla, G. Kumar, P. Singh, V. Luxami… S. Kumar.** (2020). Chemodosimeters for optical detection of fluoride anion, *Coord. Chem. Rev., 405* 213138.

[75**] B.R. Jali, J.B. Baruah**. (2021) Recent progress in Schiff bases in detections of fluoride ions, *Dyes Pigm., 194* 109575.

[76**] J. Zhao, H. Huang, W. Zhou, D. Wu, J. Xia.** (2021) Synthesis and characterization of a BN-embedded nine-ring fused heteroaromatics with dual channel detection of fluoride anions, *Dyes Pigm., 194* 109648.

[77] **M. Lee, S. Jo, D. Lee, Z. Xu, J. Yoon.** (2015) A new naphthalimide derivative as a selective fluorescent and colorimetric sensor for fluoride, cyanide and CO_2, *Dyes Pigm., 120* 288-292.

[78] **B.T. Nguyen, E.V. Anslyn.** (2006) Indicator–displacement assays, *Coord. Chem. Rev., 250* 3118-3127.

[79**] K.N. Koh, K. Araki, A. Ikeda, H. Otsuka, S. Shinkai.** (1996). Reinvestigation of Calixarene-Based Artificial-Signaling Acetylcholine Receptors Useful in Neutral Aqueous (Water/Methanol) Solution, *J. Am. Chem. Soc., 118* 755-758

[80] **I.A. Rather, R. Ali.** (2021), Indicator displacement assays: from concept to recent developments, *Org. Biomol. Chem.*

[81] **Z. Li, W. Zhao, X. Li, Y. Zhu, C. Liu, L. Wang…H. Zhang.** (2012). 18-Naphthyridine-Derived $Ni2^{+}$/$Cu2^{+}$-Selective Fluorescent Chemosensor with Different Charge Transfer Processses, *Inorg. Chem., 51* 12444-12449,

[82] **A. Baeyer,** (1886) Ueber ein Condensations product von Pyrrol mit Aceton, *Berichte der deutschen chemischen Gesellschaft, 19* 2184-2185,

[83] **A. Aydogan, A. Koca, M.K. Şener, J.L. Sessler**. (2014) EDOT-Functionalized Calix[4]pyrrole for the Electrochemical Sensing of Fluoride in Water, *Org. Lett*., *16* 3764-3767.

[84**] P.A. Gale, J.L. Sessler, V. Kral, V. Lynch.** (1996) Calix[4]pyrroles: Old yet new anion-binding agents, *J. Am. Chem. Soc*., *118* 5140-5141.

[85] **H. Miyaji, W. Sato, J.L. Sessler,** (2000) Naked-Eye Detection of Anions in Dichloromethane: Colorimetric Anion Sensors Based on Calix[4]pyrrole, *Angew. Chem., 112* 1847-1850.

[86] **S. Bähring, H.D. Root, J.L. Sessler, J.O. Jeppesen.** (2019). Tetrathiafulvalene-calix[4]pyrrole: a versatile synthetic receptor for electron-deficient planar and spherical guests, *Org. Biomol. Chem*., *17* 2594-2613.

[87] **S.K. Kim, H.G. Lee, G.I. Vargas-Zúñiga, J.H. Oh, V.M. Lynch, M.H. Lee, J.L. Sessler,** (2017) A fluorogenic calix[4]pyrrole with a small rigid strap showing different fluorescent responses to anions, *Supramol. Chem***.,** *29* 651-657.

[88] **T.K. Ghorpade, M. Patri, S.P. Mishra.** (2016). Highly sensitive colorimetric and fluorometric anion sensors based on mono and di-calix[4]pyrrole substituted diketopyrrolopyrroles, *Sens. Actuators B: Chem*., *225* 428-435.

[89] **R. Gotor, A.M. Costero, S. Gil, P. Gaviña, K. Rurack.** (2014). On the Ion-Pair Recognition and Indication Features of a Fluorescent Heteroditopic Host Based on a BODIPY Core, *Eur. J. Org. Chem*., 4005-4013.

[90] **A.S.F. Farinha, M.R.C. Fernandes, A.C. Tomé.** (2014). Chromogenic anion molecular probes based on β,β'-disubstituted calix[4]pyrroles, *Sens. Actuators B*: Chem., *200* 332-338,

[91] **P. Thiampanya, N. Muangsin, B. Pulpoka**. (2012). Azocalix[4]arene Strapped Calix[4]pyrrole: A Confirmable Fluoride Sensor, *Org. Lett*., *14*

[92] **P.A. Gale, L.J. Twyman, C.I. Handlin, J.L. Sessler.** (1999). A colourimetric calix[4]pyrrole-4-nitrophenolate based anion sensor, *Chem. Commun*., 1851-1852.

[93] **M.M. Linn, D.C. Poncio, V.G. Machado.** (2007) An anionic chromogenic sensor based on the competition between the anion and a merocyanine solvatochromic dye for calix[4]pyrrole as a receptor site, *Tetrahedron Lett*., *48* 4547-4551.

[94] **P. Sokkalingam, J. Yoo, H. Hwang, P.H. Lee, Y.M. Jung, C.-H. Lee.** (2011) Salt (LiF) Regulated Fluorescence Switching, *Eur. J. Org. Chem*., 2911-2915.

[95**] D. Sareen, J.H. Lee, H. Hwang, S. Yoo, C.-H. Lee**. (2016). Ion-mediated single-molecular optical switching and sensing based on the fluorophore-tethered calix[4]pyrrole, *Chem. Commun*., *52* 5852-5855,

[96] **R.F. Chen**. (1968). FluorescentpH Indicator. Spectral Changes of 4-Methylumbelliferone, *Anal. Lett*., *1* 423-428,

[97] **N. Klonis, A.H.A. Clayton, E.W. Voss Jr., W.H. Sawyer.** (1998). Spectral Properties of Fluorescein in Solvent-Water Mixtures: Applications as a Probe of Hydrogen Bonding Environments in Biological Systems, Photochem. Photobiol., *67* 500-510.

[98] **A. Aydogan, J.L. Sessler, A. Akar, V. Lynch,** (2008) Calix[4]pyrroles with long alkyl chains: Synthesis, characterization, and anion binding studies, *Supramol. Chem.*, *20* (1−2), 11-21.

[99**] H.-M. Chen, S.A. Nasseri, P. Rahfeld, J.F. Wardman, M. Kohsiek, S.G. Withers**. (2021) Synthesis and evaluation of sensitive coumarin-based fluorogenic substrates for discovery of α-N-acetyl galactosaminidases through droplet-based screening, *Org. Biomol. Chem*., *19* 789-793.

[100] **D. Brynn Hibbert, P. Thordarson,** (2016) The death of the Job plot, transparency, open science and online tools, uncertainty estimation methods and other developments in supramolecular chemistry data analysis, *Chem. Commun*., *52* 12792-12805.

[101] **A.F.D. de Namor, M. Shehab.** (2003). Selective recognition of halide anions by calix[4]pyrrole: A detailed thermodynamic study, *J. Phys. Chem. B, 107*

[102] **T. Ooi, H. Sugimoto, K. Doda, K. Maruoka**. (2001). Esterification of carboxylic acids catalyzed by in situ generated tetraalkylammonium fluorides, *Tetrahedron Lett., 42* 9245-9248,

[103] **I. Kuwajima, T. Murofushi, E. Nakamura**, (1976) Quaternary Ammonium Fluoride-Catalyzed Conjugate Addition of Thiols to C=C Double Bonds, *Synthesis*, 602-604,

CURRICULUM VITAE

Name Surname **:** Sana Amharar

EDUCATION:

- **B.Sc.** **:** 2010, University of ROUEN, Science and technology Faculty, Chemistry,
- **M.Sc.** **:** 2012, University of ROUEN, Chemistry

PROFESSIONAL EXPERIENCE:

- 2006 FRANCE, Laboratory technician, SGS Multilab, St Etienne du Rouvray

PUBLICATIONS :

- **Sana Amharar,** Samet Yuvayapan and Abdullah Aydogan**.** 2018**.** A thermoresponsive supramolecular polymer gel from a heteroditopic calix[4]pyrrole, *Chemical Communication* vol 54, 829-932.
- **Sana Amharar,** Armağan Atsay, Abdullah Aydoğan. 2020. Ion pair recognition based supramolecular polymer showing rapid and reversible Sol-Gel transition through Van deer Waals interaction, *ACS Applied Polymer Materiel*, 2, 5371-5376.
- **Sana Amharar,** Abdullah Aydoğan.2022. Highly sensitive and cost-effective fluorescent turn-on sensors based on octamethylcalix[4]pyrrole receptor for the detection of fluoride, *Dyes and Pigments,*197, 109918.